Austrian Journal of Earth Sciences | Vienna | 2017 | Volume 110/1 | 57 - 77 | DOI: 10.17738/ajes.2017.0005

Carbonate cementation in Upper Eocene clastic reservoir rocks from the North Alpine Foreland Basin (Austria)

Marie-Louise GRUNDTNER[1)*)], Doris GROSS[1)], Reinhard GRATZER[1)], David MISCH[1)], Reinhard F. SACHSENHOFER[1)] & Lorenz SCHEUCHER[2)]

1) Department of Applied Geosciences and Geophysics, Montanuniversitaet Leoben, 8700 Leoben, Austria;

2) Rohoel-Aufsuchungs AG, Schwarzenbergplatz 16, 1015 Vienna, Austria;

*) Corresponding author, marielouise.grundtner@gmail.com

KEYWORDS North Alpine Foreland Basin; diagenesis; reservoir rock; carbonate cement; rock-fluid interaction

Abstract

A strong relationship between carbonate precipitation and microbial gas generation is evident for the Upper Eocene reservoir rocks of the North Alpine Foreland Basin. To achieve a better understanding of this relationship, 40 samples of limnic to shallow marine, gas-, oil- and water-bearing sandstones were studied to determine mineralogy and diagenetic history. The specific mineral parageneses were used to reconstruct changes in the hydrogeochemical conditions over time. Thus, authigenic mineral phases within reservoir rocks are an important archive for the reconstruction of pore fluid composition changes.

The eogenetic pore space evolution of investigated Eocene sandstones is influenced by their primary mineralogy, which is strongly controlled by (i) depositional environment, (ii) detrital input and (iii) transport distances. Thus, a low compositional maturity is associated with high feldspar and high clay mineral content. Authigenic clay minerals, formed during several stages of diagenesis, play an important role for reservoir quality, due to pore space reduction.

During eogenesis, authigenic micritic and sparitic carbonate phases are precipitated, which decreases the pore space. These eogenetic carbonate cements exhibit isotope values of about $\delta^{13}C$: -5.9 to +2.2‰ and $\delta^{18}O$: -8.3 to -4.3‰ [VPDB]. Some of these samples indicate a trend towards lighter $\delta^{18}O$ values (-17.2‰), which is attributed to meteoric flush.

Within the Eocene sandstones, two types of strongly cemented zones with low permeabilities can be differentiated: (i) extraordinary light $\delta^{13}C$ (-28.4‰) carbonates, which formed due to degradation of organic matter at the stage of advanced sulfate reduction and (ii) heavy $\delta^{13}C$ ($\delta^{13}C$: +8.7‰), which precipitated at the fermentation zone.

Within the reservoir sandstones telogenesis is characterized by mineral destabilization (e.g. carbonate and feldspar corrosion) and kaolinite precipitation. The formation of authigenic kaolinite booklets resulted into a decrease in porosity.

1. Introduction

Eocene sandstones represent the main oil reservoir in the Austrian sector of the North Alpine Foreland Basin (NAFB) (Wagner, 1980; 1996; 1998; Veron, 2005). They experienced a complex charging history, involving minor early primary microbial gas and late thermogenic oil (Gusterhuber et al., 2013, 2014). In addition, in-situ oil alteration occurs within the reservoir sandstones in shallow horizons (above -650 m; Sachsenhofer et al., 2006; Reischenbacher & Sachsenhofer, 2011; Gratzer et al., 2011). Therefore, the NAFB provides a unique opportunity to study the effect of hydrocarbon generation and its influence on the diagenetic history, which is the main aim of the present contribution.

The quality of hydrocarbon reservoirs is strongly controlled by depositional environments and related processes, as well as diagenetic evolution. Aside from the primary composition, changes in the pore fluids influence formation and dissolution of mineral phases. In general, the reservoir geometry and the influence of detrital minerals on pore space evolution is well understood (Bjørlykke, 2014). Gross et al. (2015) showed for example that eogenetic processes are strongly affected by primary composition. Amongst others, primary feldspar content and subsequent dissolution during diagenesis have a strong influence on the availability of free pore space.

However, the rock-fluid interaction in hydrocarbon systems and the influence of gas and oil on the formation of authigenic minerals is still a matter of discussion (e.g. Curtis, 1978; Surdam et al., 1989; Lundegard et al., 1992; Prochnow et al., 2006; Gorenc & Chan, 2015). The impact of fluids, especially of hydrocarbons, on pore space evolution is discussed by e.g., Bjørlykke et al. (1989) and Van Berk & Schulz (2015).

Important insights into the hydrocarbon generation and alteration of hydrocarbons are provided by stable carbon isotopic composition of authigenic carbonate minerals. The isotopic signature depends on the diagenetic carbon cycle and on the carbon source itself (Friedman & O´Neil, 1977; Curtis, 1978). In general, the initial isotope pool is modified by different processes during diagenesis, like microbial oxidation, microbial sulfate reduction, fermentation and thermally-induced decarboxylation (Irwin et al., 1977; Irwin & Hurst, 1983). Furthermore, $\delta^{18}O$ ratios reflect changes in water conditions at time of formation, such as precipitation temperature and primary isotopic composition (Friedman & O´Neil, 1977; Irwin et al., 1977). In general, $\delta^{13}C$ is relatively stable during diagenetic processes, while $\delta^{18}O$ is more sensitive to exchange reactions (Aharon, 2000).

2. Geological setting

The NAFB extends from Geneva (Switzerland) to Vienna (Austria) along the northern margin of the Alps (Fig.1a). As a result of the Paleogene Alpine orogeny, the foreland basin was formed between the European plate (Bohemian Massif) in the North, and the overthrust units of the Eastern Alps to the South (Roeder & Bachmann, 1996; Sissingh, 1997; Wagner, 1996, 1998) (Fig.1a). Due to thrust loading, the basin shows an asymmetric geometry (Fig.1b).

The basement of the Mesozoic pre-foreland basin sediments is formed by Variscian metamorphic rocks of the Bohemian Massif and local Permo-Carboniferous graben sediments. During Mesozoic times, shallow marine siliciclastics and carbonate rocks were deposited (Wagner, 1996, 1998).

The foreland basin stage commenced in Late Eocene times (e.g. Bachmann et al., 1987), when limnic-fluviatile and shallow marine sandstones, mudstones and carbonate rocks were deposited. Rapid subsidence in Early Oligocene times resulted in the deposition of the deep marine sediments (Schöneck to Zupfing formations). Deep marine conditions prevailed until the Early Miocene east of Munich. In Middle and Late Miocene times, a transition from a deep marine to a freshwater depositional setting developed (Fig. 2).

2.1 Sedimentary successions in the study area

The Upper Eocene (Priabonian) rocks of the Austrian Alpine Foreland Basin reach a maximum thickness of about 120 m. According to Wagner (1998), they comprise from bottom to top (Figs. 2,3):

- Terrestrial sediments of the Voitsdorf Formation (former Limnic Series after Wagner (1980, 1998)) with varicolored mudstones, bright-grey fluvial to deltaic sandstones and thin coal seams.

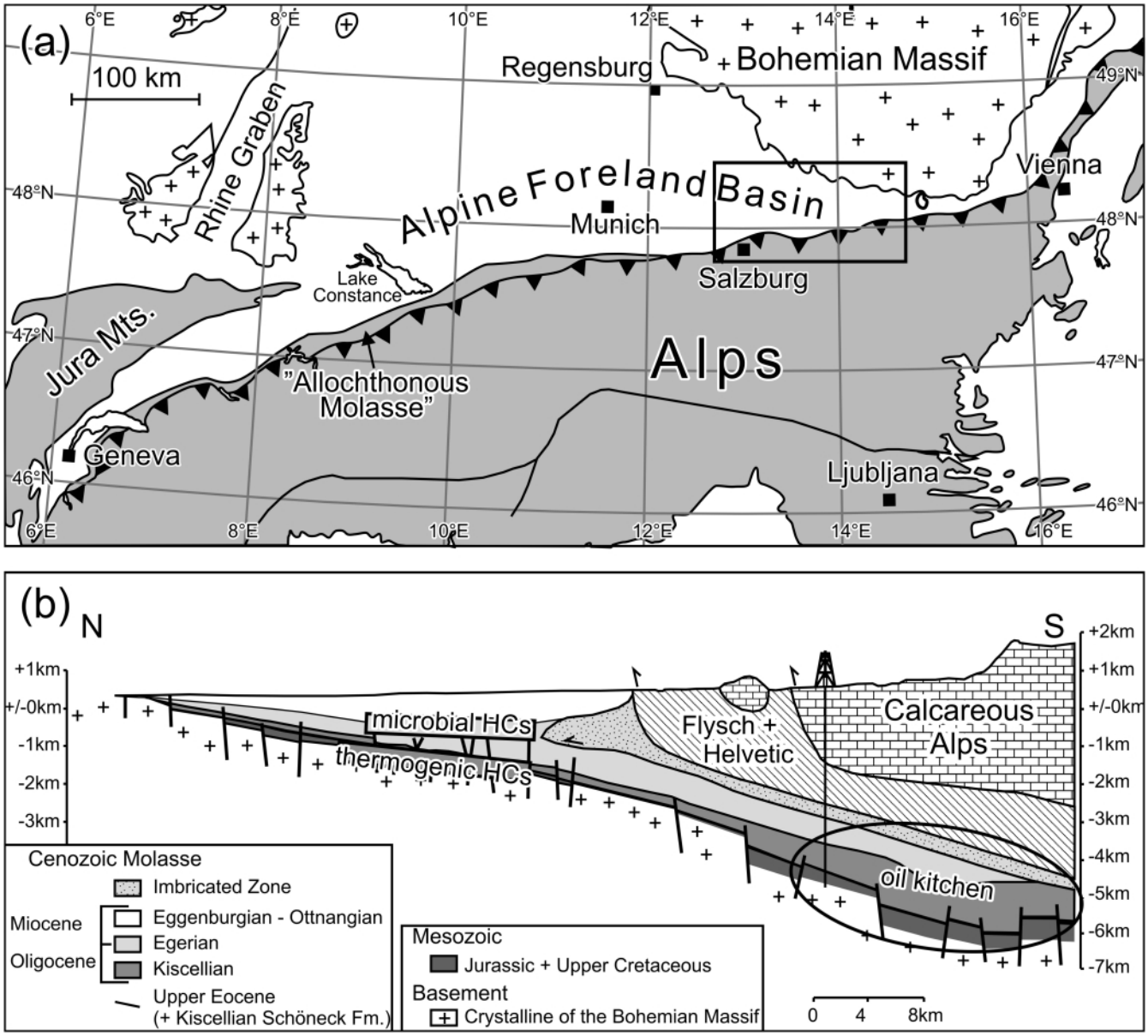

Figure 1: a) Sketch map of the North Alpine Foreland Basin. The black rectangle marks the study area. b) N-S trending cross section through the NAFB with its two petroleum systems (HCs: hydrocarbons) (after Sachsenhofer & Schulz, 2006).

- Brackish-water Cerithian Beds, characterized by fossil-rich dark-grey mudstones with sandstone bodies, interpreted as tidal channel fills (Wagner, 1980, 1998).
- Shallow marine, often bioturbated, sandstones of the Ampfing Formation (former Sandsteinstufe after Wagner (1980, 1998)).
- *Lithothamnium* Limestone containing red algal reef carbonates and their debris.

Open marine *Nummulitic* Sandstone, *Discocyclina* limestone, marls of the Perwang Formation and *Globigerina* Limestone developed in southwestern direction (Wagner, 1998).

A northeastward-directed transgression caused a shift of Eocene facies zones towards east-northeast (Malzer et. al., 1993; Wagner, 1998; Rasser & Piller, 2004). The facies distribution during deposition of the upper part of the *Lithothamnium* Limestone is shown in Fig. 3.

2.2 Hydrocarbon system

Within the Austrian sector of the NAFB, a thermogenic and a microbial petroleum system can be distinguished:

1) Lower Oligocene deep-water sediments (Schöneck, Dynow, Eggerding formations; Schulz et al. 2002; Sachsenhofer & Schulz, 2006; Sachsenhofer et al. 2010) are the main source rocks of the thermogenic petroleum system with oil and minor thermogenic gas. Hydrocarbon generation started in Miocene times, when the Alpine nappes started to overthrust the southern NAFB and ended about 5 Ma ago due to uplift and cooling (Gusterhuber et al., 2013, 2014). The oil window is reached at a depth of about 4 to 6 km below sea level. The expelled gas and oil migrated laterally northwards into Mesozoic and Cenozoic reservoir rocks, including Eocene fluviatile (Voitsdorf Formation), tidal (Cerithian Beds) and shallow marine deposits (Ampfing Formation, *Lithothamnium* Limestone) (Schmidt & Erdogan, 1996; Bechtel et al., 2013). Hydrocarbon accumulations also occur in Cenomanian sediments of the autochthonous Mesozoic cover on top of the Bohemian Massif and Lower Oligocene sandstones and conglomerates.

The total thickness of Upper Eocene sandstones ranges between 10 and 15 m, with 30 m at maximum. Porosity varies from 12 – 25 % and permeability from a few mD up to 2000 mD (Malzer et al. 1993; Wagner, 1998). The best carrier rocks are coastal sandstones located in the East of the basin (Wagner, 1980). With the exception of shallow biodegraded deposits, the API gravity typically varies between 30 and 35 classifying a light oil (Gratzer et al., 2011).

2) The Oligocene-Miocene petroleum system comprises microbial gas, which has been generated in deep marine pelitic rocks of the Puchkirchen and Hall formations and migrated into sandstones and conglomerates of the same units (Schulz et al., 2009). Molecular and isotopic data indicate a mixing of thermogenic and microbial gases (Reischenbacher and Sachsenhofer 2011).

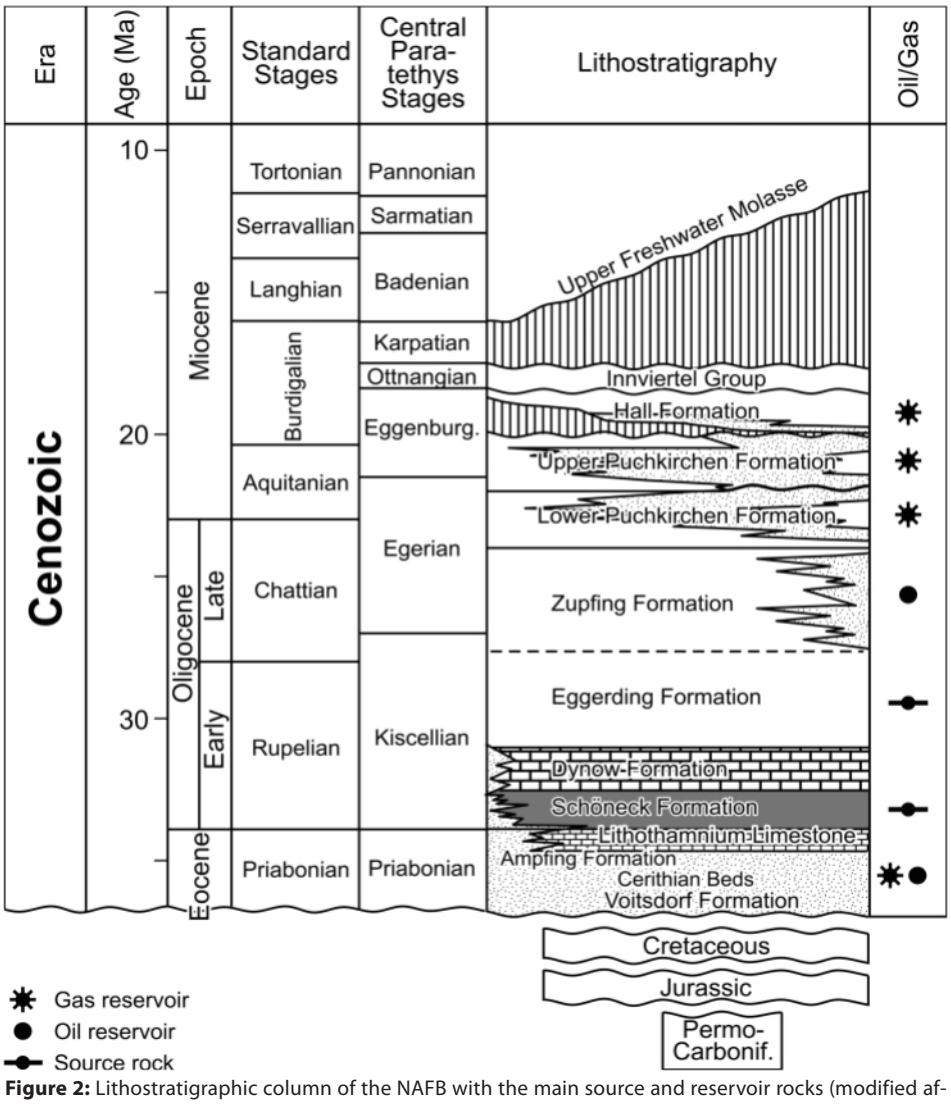

Figure 2: Lithostratigraphic column of the NAFB with the main source and reservoir rocks (modified after Wagner, 1998 and Grunert et al., 2015).

3. Samples and Methods

A total of 40 core samples from Eocene reservoir units have been selected for the present study. The investigated core intervals comprise lengths of 10 to 18 m. On average, 3 samples per sandstone layer were taken. The samp-

les cover a depth range of 1500 to 2000 m below sea level. In order to enable the investigation of rock-fluid interactions in zones with different pore fluids, samples from gas-, oil- and water-bearing sections have been taken. Core gamma ray spectrometry was applied to determine the core-to-log shift and thus, to precisely locate fluid contacts.

Cores were provided by RAG and represent Voitsdorf Formation, Cerithian Beds and Ampfing Formation. The investigated sandstone samples are listed referring to pore filling and stratigraphic unit:

- Gas cap, oil zone, oil-water contact, gas-water contact:
  - 1 well from Voitsdorf Formation (well F)
  - 2 wells from Cerithian Beds (wells F, G)
  - 6 wells from Ampfing Formation (wells A, B, C, D, E, H)
- Strongly carbonate cemented:
  - 1 well from Voitsdorf Formation (well F)
  - 1 well from Cerithian Beds (well G)
  - 2 wells from Ampfing Formation (wells B, H)

Thin sections were prepared for all samples, embedded in blue colored epoxy resin for visualization of porosity and investigated using polarized light microscopy. The mineralogical composition of the sandstones was evaluated by point counting of 300 points per thin section.

Polished and carbon-coated thin sections were investigated with a Superprobe JEOL JXA 8200 electron microprobe. Energy dispersive X-ray (EDX) analysis supported the mineral identification. In addition, element mapping of Na, Mg, Al, Si, K, Mn and Fe of selected areas by wavelength dispersive X-ray (WDX) facilitated the visualization of mineral phase distributions.

Pore space evaluation was carried out using a Zeiss Evo MA 15 scanning electron microscope (SEM) with an Inca Dry Cool EDX spectrometer. The acceleration voltage amounts to 15 or 20 kV and the beam current to 10 nA. Small carbon-coated split samples were used. SEM analysis is the key method for the reconstruction of diagenetic parasequences, because mineral grains, pore space and their filling are identified in-situ (Tucker, 1996). With this technique, clay mineral morphologies are visualized and thus clay minerals can be distinguished. Moreover, it is possible to detect different generations of mineral overgrowths.

Qualitative and semi-quantitative bulk rock compositions of all samples was determined by X-ray diffraction analysis (XRD) as the basic analysis method for clay minerals (Tucker, 1996). Thereby, the samples were ground manually in an agate mill to a fine powder and analyzed texture-free with a Panalytical X'Pert diffractometer (CuKα-radiation; 35 kV, 35 mA, step size 0.0167°, 20 s per step, 67-2° 2θ). Qualitative analysis was done based on the JCPDS table (1974), Brindley (1980) and Moore & Reynolds (1997), and semi-quantitative analysis was performed using the software of ADM-V7, RMS Kempten.

The identification of clay minerals with the XRD analysis supports the measurements of the pore filling made by EDX

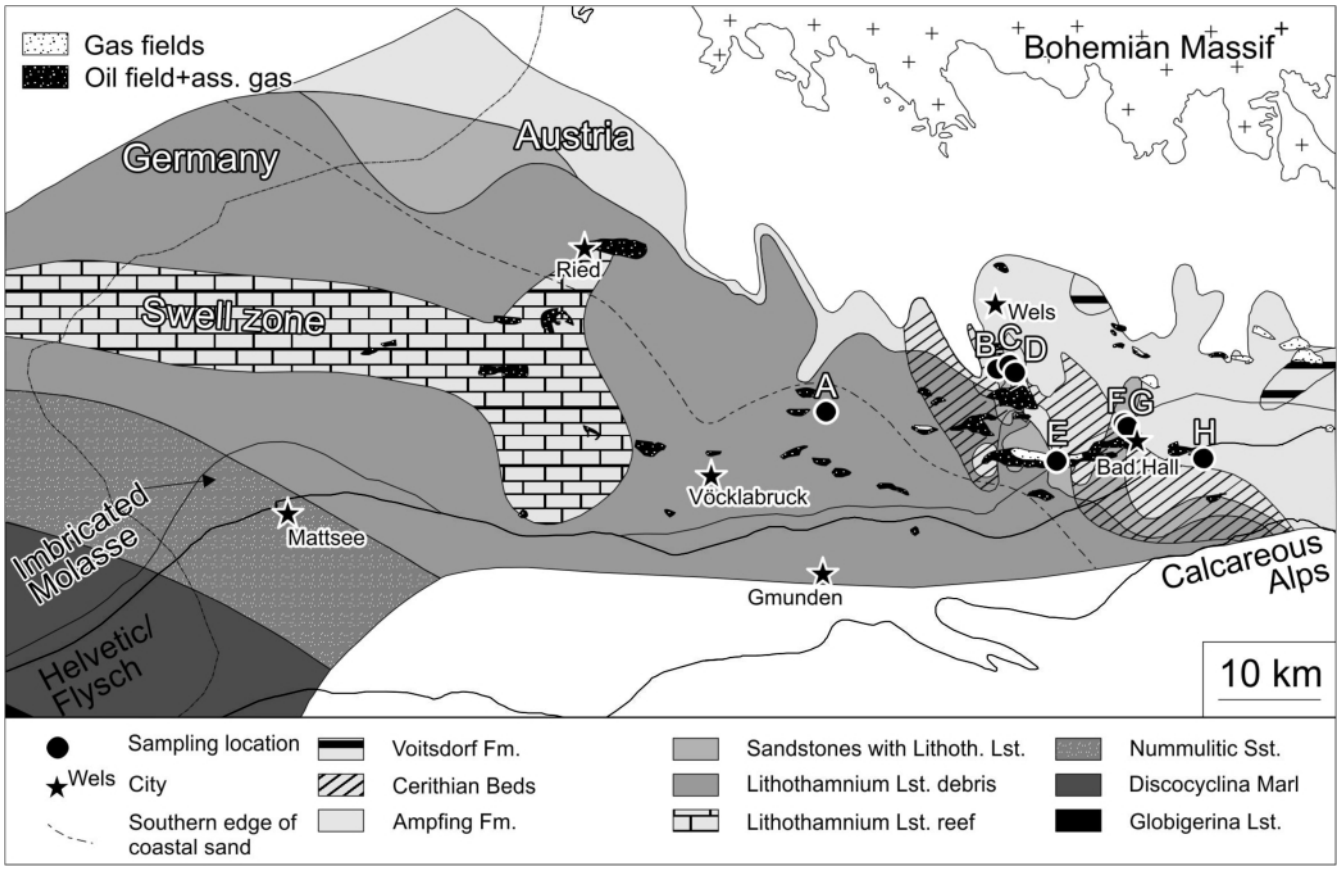

Figure 3: Upper Eocene facies distribution in the NAFB during deposition of the Upper Lithothamnium Limestone (after Wagner, 1980) and the location of Eocene gas and oil fields and sampled wells (A-H).

analysis the electron microprobe and SEM.

All presented mineral amounts (vol%) are based on the average from point counting and semi-quantitative XRD analysis.

Stable isotope ratios of carbon ($\delta^{13}C$) and oxygen ($\delta^{18}O$) were measured mainly on carbonate cements. The necessary amount of sample powder depends on the carbonate content, which was estimated from the semi-quantitative XRD analysis. According to this, 0.2 mg of sample mass correspond to a pure carbonate rock, whereas the sample mass was increased for rocks with a mixed siliciclastic/carbonatic composition, following a linear trend. Samples were dissolved in concentrated phosphoric acid (H_3PO_4), and heated to 70 °C in an online system (Gasbench II with carbonate option). The analysis was carried out with a ThermoFisher DELTA V isotope ratio mass spectrometer (Delta VIRMS). The results were then normalized to the Vienna Pee Dee Belemnite (VPDB) standard; data have a standard deviation of 0.2 % for $\delta^{13}C$ and 0.8 % for $\delta^{18}O$.

4. Results

In this section, the mineralogy, as well as the isotopic signature of authigenic carbonate cements is described separately for investigated rocks from each stratigraphic unit, with respect to diagenetic mineral precipitation/dissolution caused by different pore fluids. An overview of the investigated core intervals is given in Fig. 4.

4.1 Petrology

4.1.1 Voitsdorf Formation

The Voitsdorf Formation comprises non-marine mudstones and sandstones. Sandstones of the studied core intervals show a mean thickness of 2 m and are medium-grained and locally carbonate-cemented (Fig. 5a). They are interbedded with dark-grey mudstone horizons, which occasionally host dispersed and coarse-grained quartz grains (Figs. 4).

Detrital grains are angular, poorly sorted, and show a low sphericity. The main components are quartz (40 vol%) and feldspar (18 vol%). Quartz occurs as monocrystalline (28 vol%) and minor polycrystalline (12 vol%) grains. Alkali feldspar (17 vol%) dominates over plagioclase (1 vol%), further the amount of albite is higher than anorthite. Detrital muscovite, biotite (5 vol%) and some lithic fragments (7 vol%) occur in minor amounts. The lithic fragments are predominantly of metamorphic origin (e.g. mica schists). Sandstones of the Voitsdorf Formation are classified as lithic arkoses, according to Folk´s classification (Folk, 1974) (Fig. 7). The average clay mineral content (kaolinite, illite, and chlorite (penninite)) is 10 vol%, carbonate cements amount to 5 vol% in a few samples. The porosity and permeability average 15 % and 400 mD, respectively.

4.1.2 Sandstones of Cerithian Beds

The studied reservoir rocks of the Cerithian Beds are in average 4 m thick and consist of coarse-grained sandstones embedded in fossil-rich dark-grey mudstones. Grains are typically angular and show a high sphericity, with moderate to poor sorting. Quartz (41 vol%) and feldspar (21 vol%) are the main components. Monocrystalline quartz (26 vol%) prevails over polycrystalline quartz (15 vol%), whereas alkali feldspar (19 vol%) is more common than plagioclase (2 vol%, mainly albite). Lithic fragments amount 10 vol%, whereas pyrite, iron oxides, clay minerals and mica are present in amounts of up to 6 vol% (Fig. 6). Consequently, the sandstones are classified as lithic arkoses after Folk (1974) (Fig. 7). Sandstones of the Cerithian Beds show an average porosity of 15 % (17 – 20 %) and permeability of 1350 mD (790 – 1900 mD).

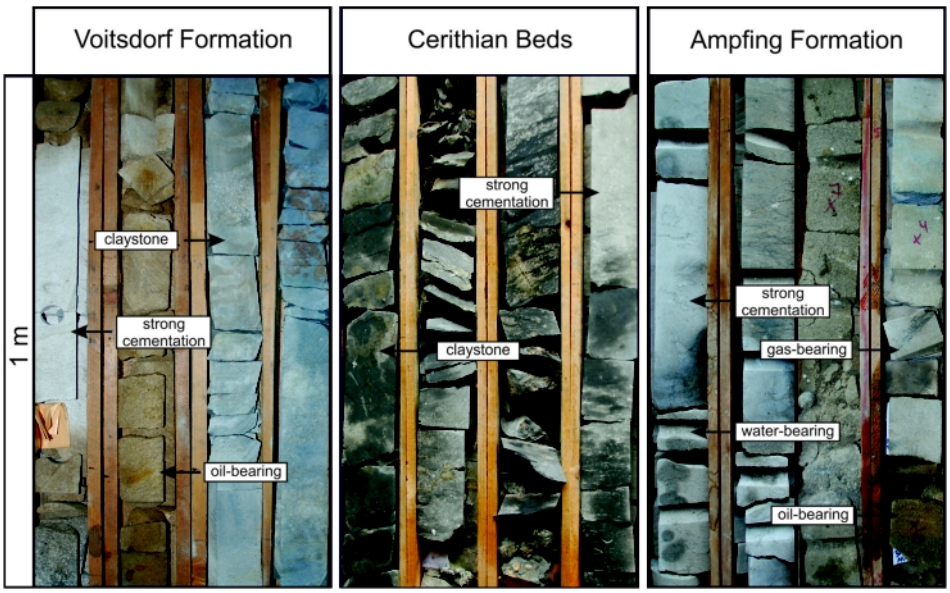

Figure 4: Overview of core boxes: The bottom of the core boxes is left, the top in the right upper corner. Left: Voitsdorf Formation with strongly cemented and oil-bearing coarse-grained sandstones embedded within varicolored mudstones (ca. 1810 m below ground level). Centre: Cerithian Beds with strongly cemented, coarse-grained sandstone in dark-grey, fossiliferous mudstones (ca. 1870 m). Right: Ampfing Formation with water-bearing and strongly cemented medium-grained sandstones (left) (ca. 1660 m) and oil- and gas-bearing sandstones (right) (ca. 1580 m).

4.1.3 Ampfing Formation

Investigated sandstones of the Ampfing Formation are medium-grained and up to 6 m thick (Fig. 5b). The moderately sorted grains are angular and exhibit high sphericity. The main mineral phases are quartz (42 vol% total; 27 vol% monocrystalline; 15 vol% polycrystalline) and feldspar (15 vol% total; 12 vol% alkali feldspar; 3 vol% plagioclase). Lithic fragments (11 vol%) are mainly of metamorphic origin. The partially increased con-

tents of muscovite and biotite (7 vol%) are likely to result from the disintegration of mica schists. Clay minerals and carbonate cement are present in considerable amounts (8 vol% and 5 vol%, respectively). Foraminifera are rare, but their presence supports the marine depositional environment. According to Folk´s classification (Folk, 1974), most of the Ampfing sandstones are lithic arkoses. Samples, which are located in the northern part of the NAFB, can be classified as feldspatic litharenites, minor subarkoses and sublitharenites (Fig. 7). The porosity of these sandstones averages 12 % (7 - 17 %), while the mean permeability is 140 mD (3 – 570 mD). Sandstones of the Ampfing Formation show a higher compositional maturity than the underlying sandstones of Cerithian Beds and Voitsdorf Formation.

4.2 Diagenetic minerals

4.2.1 Water-bearing sandstones

Glauconite, representing the earliest diagenetic (authigenic) phase, is present in the water-bearing samples from the Ampfing Formation and is characterized by dark green to brownish green colors, indicating partial alteration into berthierine. Locally, detrital grains are surrounded by diagenetic clay mineral rims or carbonate cements. Based on their paragenetic relationship, which was observed under microscope, it is evident that the clay minerals formed first, followed by the carbonate cements (Figs. 8a,b). The eogenetic clay minerals were identified as illite, smectite and kaolinite, and are present in total amounts of 10 vol%. These clay minerals were identified by characteristic EDX spectra at electron microprobe and SEM analysis. Si, Al, and K peaks are prevailing at these measured spectra. Therefore the dominance of illite is deduced. Furthermore, partial dissolution of feldspar (especially albite) and replacement by clay minerals (kaolinite, illite) is evident.

Some quartz grains show corroded margins and are covered by a micritic cement generation (CcI), which is partly replaced by a later, sparitic one (CcII) (Fig. 9a). Both cement types together account for 5 vol% in the investigated samples. The sparitic cement appears as coarse aggregates of mm-size and shows a clear granular morphology. Relatively older calcite cements are often strongly corroded, if they are in contact with younger authigenic illite. Illite forms booklets growing into open pore space, which mark the last diagenetic stage within the water-bearing sandstones (Fig. 9b).

4.2.2 Hydrocarbon-bearing sandstones

An overview of the mineralogy and texture of the oil-bearing Voitsdorf Formation, Cerithian Beds and the Ampfing Formation is given in Figs. 10 and 8, respectively. Gas-bearing sandstone intervals from the Cerithian Beds (Figs. 10g,h) and the Ampfing Formation (Figs. 8g,h) have been studied. As both gas- and oil-bearing zones show similar diagenetic mineral precipitation/dissolution, they are presented together.

Eogenetic glauconite and its alteration products are restricted to the Ampfing Formation. Brownish-colored clay minerals, illite with some smectite, iron oxides or undifferentiated fine-grained matrix, formed at the pore throats (Fig. 9e) and occurs in all investigated formations in minor amounts (5 vol%). The mineralogical composition of the brownish clay

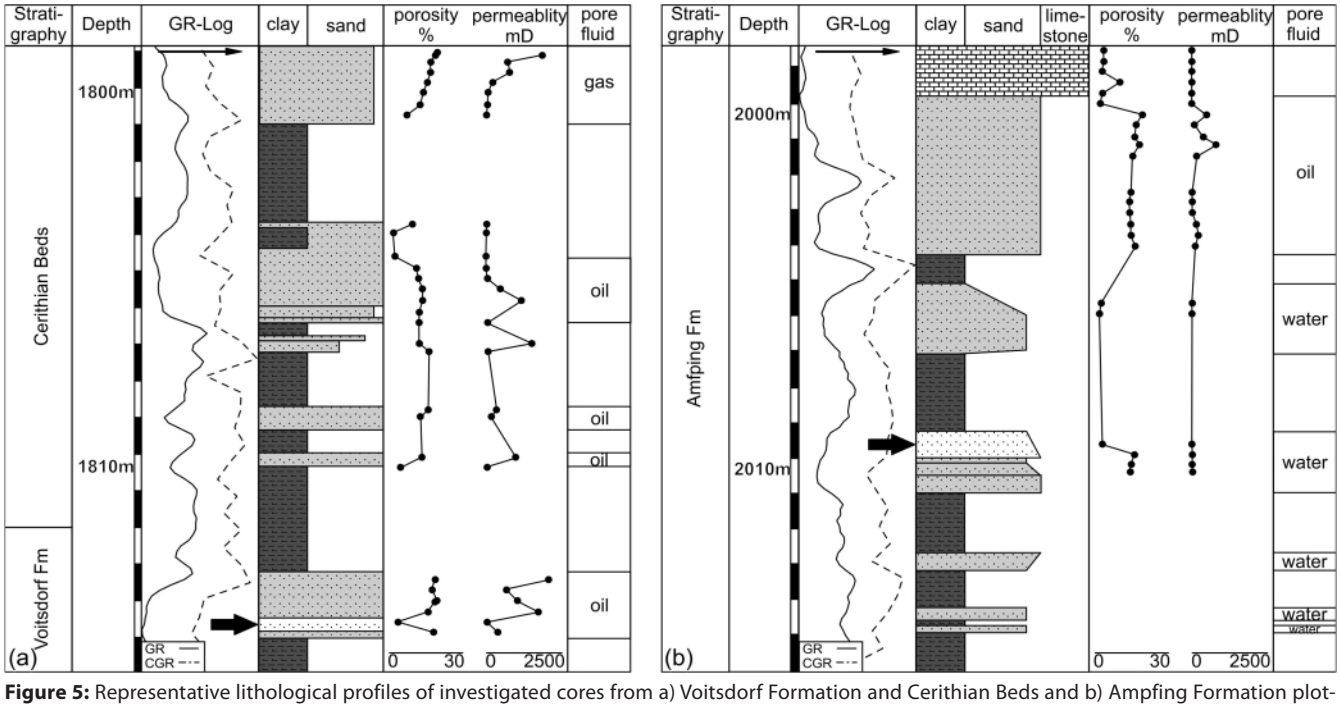

Figure 5: Representative lithological profiles of investigated cores from a) Voitsdorf Formation and Cerithian Beds and b) Ampfing Formation plotted together with porosity, permeability, and pore fluid content. Sandstones with reduced porosity due to strong carbonate cementation are colored in white and marked with a black arrow. GR: gamma ray log; CGR: measured core gamma ray. The data points from petrophysical measurements correspond to sample position.

minerals was identified by EDX and WDX electron microprobe analysis.

The growth of siderite within biotite is a characteristic dia--genetic feature for the Voitsdorf Formation and also appears, less frequently, within the sandstones of Cerithian Beds, but is missing in the Ampfing Formation. Occasionally, these siderites were identified by EDX and WDX measurements with the electron microprobe and form well defined rhombs within the Voitsdorf Formation and sandstones of the Cerithian Beds (Fig. 11a). Very eogenetic acicular carbonate rims occur in gas-bearing Cerithian Beds.

In all three formations, feldspar and, to some extent, quartz show dissolution fabrics. Partial dissolution of alkali feldspar causes authigenic clay mineral formation (kaolinite) (Fig. 11a). The partial disintegration and replacement of alkali feldspar by calcite, as shown in Fig. 11e, generates secondary porosity.

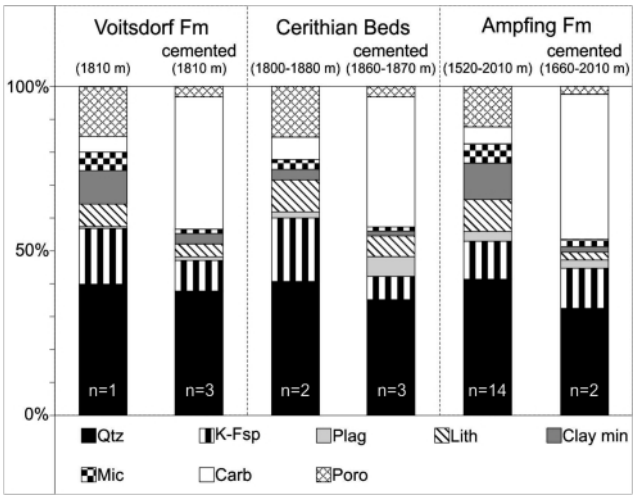

Figure 6: Average mineralogical composition and porosity of investigated samples from Voitsdorf Formation, sandstones of Cerithian Beds and Ampfing Formation. Reservoir sandstones (left column) and strongly cemented sandstones (right column) are plotted separately. Qtz_{mono}: monocrystalline quartz; Qtz_{poly}: polycrystalline quartz, K-fsp: alkali feldspar; Plag: plagioclase; Lith: lithic fragments, Clay min: clay minerals; Mic: mica; Carb: carbonate; Poro: porosity

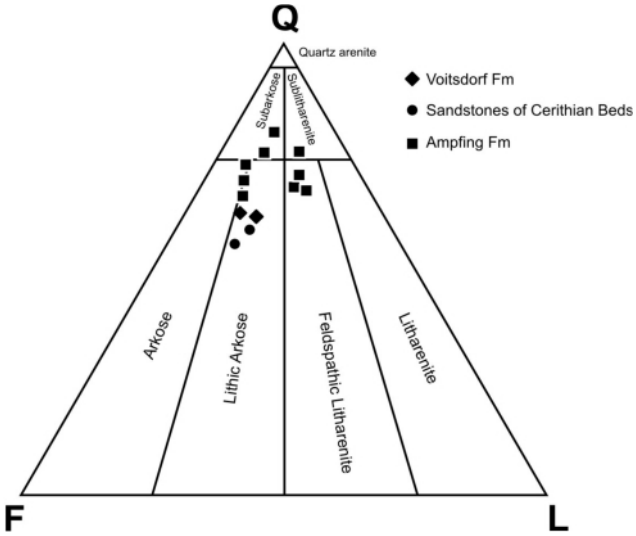

Figure 7: Ternary classification plot for clastic rocks after Folk (1974), showing non-cemented samples from the investigated stratigraphic units.

As for the water-bearing equivalents, two calcite cement types (CcI and CcII) are also present in the hydrocarbon-bearing reservoir sandstones. Again, the micritic cement is again replaced locally by the sparitic one. Both cement types are mostly present in minor amounts (5 vol%). Samples from the Voitsdorf Formation comprise the lowest average in authigenic carbonate content, whereas sediments from the Cerithian Beds host the highest amount of carbonates. These carbonate cements are recrystallized and show corrosion marks, where they appear near illite or kaolinite. The replacement of carbonate cement CcI by kaolinite is obvious in both, the oil-bearing (Fig. 11g) and the gas-bearing zones (Fig. 11h) of all investigated reservoir sections.

The presence of different generations of clay minerals within the hydrocarbon-bearing sandstones is evident. Brownish clay minerals form rims within open pores, whereas illite (Fig. 9e) and kaolinite (Fig. 11b,h,g) are prevalent in pore centers. The abundance in illite is supported by element mapping of K-contents. Figure 9f shows that the margins of the clay mineral accumulation bear the highest K-content (illite). Besides EDX measurement, illite is characterized by fibrous morphology and thus can be differentiated by the booklet structure of kaolinite at SEM analysis (see also Welton, 2003). Although kaolinite booklets of 20 µm in size were commonly observed in most samples under microscope (e.g. Fig 11a), large illite booklets (about 70 µm) appear within in the gas-bearing samples of the Ampfing Formation (Fig. 9e).

Kaolinite booklets, growing into open pore space, are the most characteristic authigenic mineral phase within gas- and oil-bearing sandstones of all horizons (Fig. 9g, 11b). In addition, kaolinite growing on the surface of alkali feldspar is also visible in SEM pictures (e.g. Fig. 9h). Kaolinite is clearly identifiably by its typical booklet morphology and the lack of K in the EDX spectrum. In comparison to the Ampfing sandstones, the kaolinite of the Cerithian Beds shows a quite common (smaller) size and some of the grain margins in the Cerithian Beds are covered with kaolinite and pyrite (Fig. 11f). The presence of these two minerals was identified by EDX measurements with the electron microprobe. Some of the larger booklets in Ampfing sandstones show interference colors similar to those of muscovite under polarized light (Figs. 8g,h).

4.2.3 Carbonate-cemented sandstones within the oil- and water-bearing zones

Strongly carbonate-cemented sandstones, between 0.1 and 0.5 m thick, occur (i) either within the water-bearing zone (Ampfing Formation) or (ii) within the oil-bearing horizon (Voitsdorf Formation). In these intervals, carbonate cementation significantly reduces the porosity. Such cementation patterns do not exist in the gas-bearing zone. Cemented sandstones in the water-bearing zone appear gray, those in the oil-bearing zone appear white (Fig. 4,5).

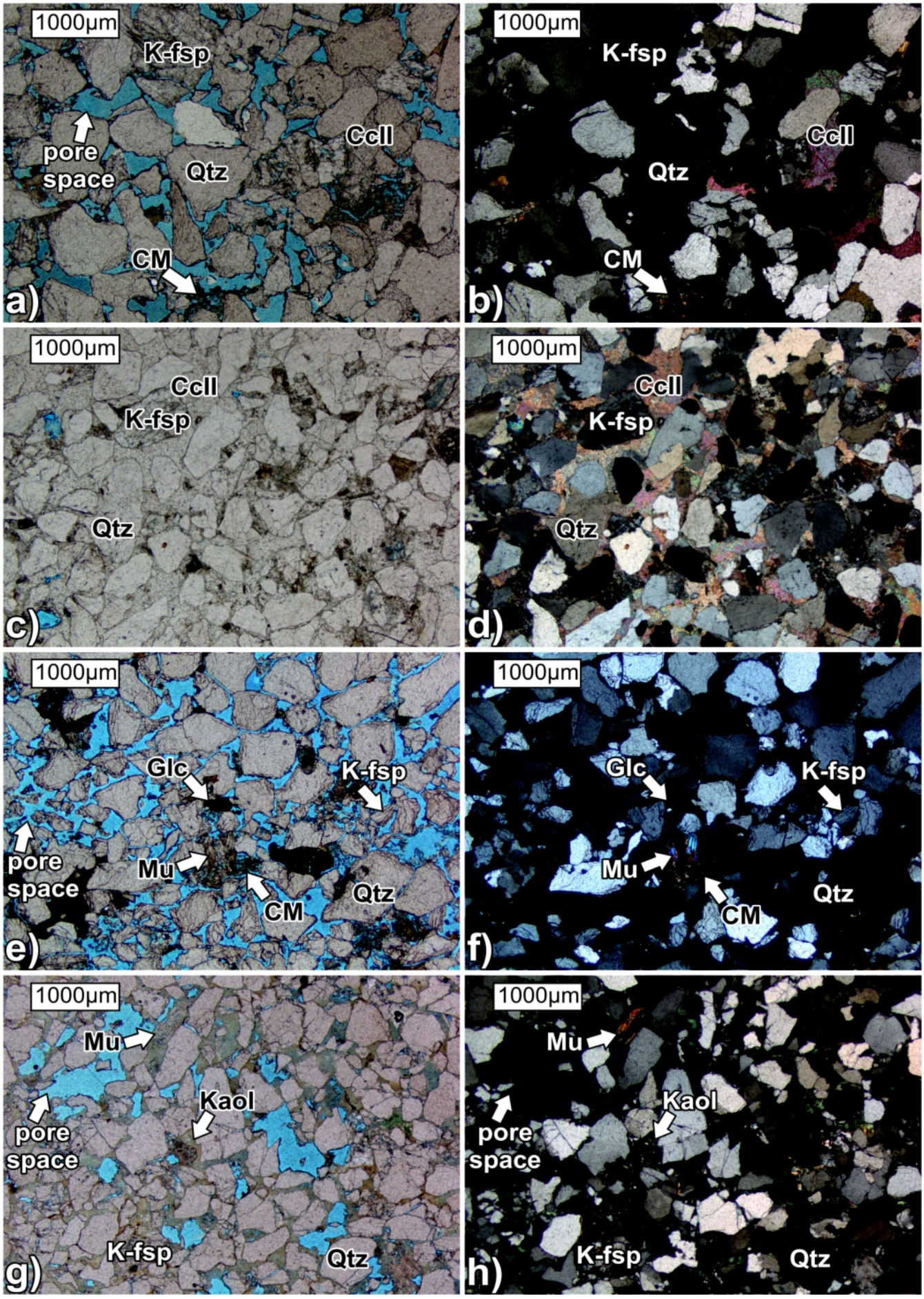
1000µm
K-fsp
pore space
Qtz
CcII
CM
a)
1000µm
K-fsp
CcII
Qtz
CM
b)
1000µm
CcII
K-fsp
Qtz
c)
1000µm
CcII
K-fsp
Qtz
d)
1000µm
Glc
K-fsp
pore space
Mu
CM
Qtz
e)
1000µm
Glc
K-fsp
Mu
CM
Qtz
f)
1000µm
Mu
Kaol
pore space
K-fsp
Qtz
g)
1000µm
Mu
Kaol
pore space
K-fsp
Qtz
h)

Glauconite is again present in samples of the Ampfing Formation exclusively, whereas clay minerals in all strongly cemented horizons are generally rare (about 3 vol% on average). Occasionally, kaolinite accumulated in grain interstices within the investigated samples, which was regularly observed under optical light and affirmed by EDX measurement with electron microprobe.

The siderite-biotite intergrowth is evident in strongly cemented rocks of the Voitsdorf Formation (Fig. 11d), which is also present in the less cemented gas- and oil-bearing sandstones of the same facies zones. In all strongly cemented horizons, quartz, and some glauconite grains in the Ampfing Formation, are corroded and feldspar is largely replaced by calcite cement. Thereby, albite is most affected; alkali feldspar displays strongly altered rims. The type of feldspar and carbonate was identified by EDX and WDX measurement with electron microprobe.

Within the strongly cemented sandstones, micritic cement (CcI) occurs locally around detrital grains, especially in areas with poor grain sorting. However, sparitic calcite (CcII) predominates and grades occasionally into poikilitic cement (pCc; Fig. 11c). Calcite is the only carbonate cement phase in the Voitsdorf Formation (Figs. 10c,d) and the Ampfing Formation (Figs. 8c,d; 9c), according to XRD, EDX and WDX analysis with electron microprobe. The percentage of carbonate cement reaches 40 vol% in cemented samples of the Voitsdorf Formation and 45 vol% in cemented samples of the Ampfing Formation. Calcite occurs as the main pore filler between detrital grains in SEM pictures (Fig. 9d). WDX element maps show slightly increased Mg contents in the pervasive calcite cements (CcII-a) of strongly cemented Ampfing sandstones (wells G and H), whereas elevated Fe contents are visible in pervasive calcite cements (CcII-b) of equivalents from the Voitsdorf Formation (well F). In addition, detrital grains from the strongly cemented sandstones of the Voitsdorf Formation (well F) exhibit comparatively more compaction than equal samples from the Ampfing Formation.

4.3 Isotopic composition

The stable carbon ($\delta^{13}C$) and oxygen ($\delta^{18}O$) isotopic composition of carbonate fractions from bulk rock samples, containing preserved fossils as well as various authigenic carbonate generations, was determined. $\delta^{18}O$ was cross-plotted with $\delta^{13}C$, and samples were grouped according to their pore filling (gas/oil/water/cement) and stratigraphic unit. Four clusters (carbonate isotope groups 1-4; see Fig. 12) were identified:

Porous sandstones correspond to the carbonate isotope groups 1 and 4. They do not show any significant differences in diagenetic minerals under the microscope. A trend between $\delta^{13}C$ and prevailing cement type (CcI and CcII, respectively) was observed in gas-, oil- and water-bearing sandstones. An increasing amount of CcII in comparison to CcI is accompanied by lighter $\delta^{13}C$.

Strongly cemented sandstones plot into two groups (carbonate isotope group 2 and 3), which are completely different from each other. Strongly cemented samples involve up to 45 vol% calcite (CcII-a and CcII-b) and are of black color in Fig. 12. CcII-a is related to lighter $\delta^{13}C$, and CcII-b causes a shift to heavier $\delta^{13}C$.

Figure 8: Thin section photographs in plane- and cross-polarized light of different samples from the Ampfing Formation: a,b) one sample from the water-bearing sandstone; c,d) one sample from the cemented sandstone; e,f) one sample from the oil-bearing sandstone; g,h) one sample from the gas-bearing sandstone (Qtz: quartz; K-fsp: alkali feldspar; CM: clay mineral; Cc: calcite; Mu: muscovite; Glc: glauconite; Kaol: kaolinite). Note high porosity in a,b,e,f,g,h.

5. Discussion

5.1 Influence of depositional environment on sediment petrology

The studied Upper Eocene rocks have been deposited during a transgressive event and comprise from bottom to top (i) fluviatile to deltaic (Voitsdorf Formation), (ii) tidal (Cerithian Beds) and (iii) shallow-marine sandstones (Ampfing Formation) (Malzer et. al., 1993; Wagner, 1998; Rasser & Piller, 2004). Sandstones of the non- to marginal marine Voitsdorf Formation and Cerithian Beds are located in deeper parts of the basin and occur as channel-shaped reservoir bodies. In comparison, the shallow-marine Ampfing Formation developed laterally as continuous sandy layers (Nachtmann, 1989).

The higher (initial) compositional maturity observed in the (southern) shallow-marine Ampfing Formation indicates a comparably higher transport distance from the hinterland and a continuous reworking by wave action, in relation to fluviatile/deltaic Voitsdorf Formation and brackish Cerithian Beds. Furthermore, the occurrence of glauconite and (rare) foraminifera in the Ampfing Formation point to a marine depositional environment. In contrast, Voitsdorf Formation and Cerithian Beds are comparatively less mature. Mineralogical composition and intensity of the weathering of the hinterland, and the depositional environment have a great influence on the abundance of che-mically unstable silicate minerals (e.g. detrital clay, mica, feldspar). Chemically unstable minerals are especially more abundant in the Voitsdorf Formation, indicating a short transport distance from a metamorphic hinterland (Bohemian Massif).

5.2 Diagenetic processes

5.2.1 Control mechanism of microbial gas generation on diagenetic pathways

The microbial degradation of organic matter for energy extraction is an important process for the entire diagenesis, especially for carbonate precipitation, because of the allocation of reagents and the control of pore water conditions (Eh and pH). Organic matter metabolization commences during sedimentation and gas (CH_4 and CO_2) is then generated. The generation of microbial gas regulates carbonate precipitation and dissolution within the pore space by pH change via carbonate solubility product alteration (Schulz et al., 2009; Schulz &

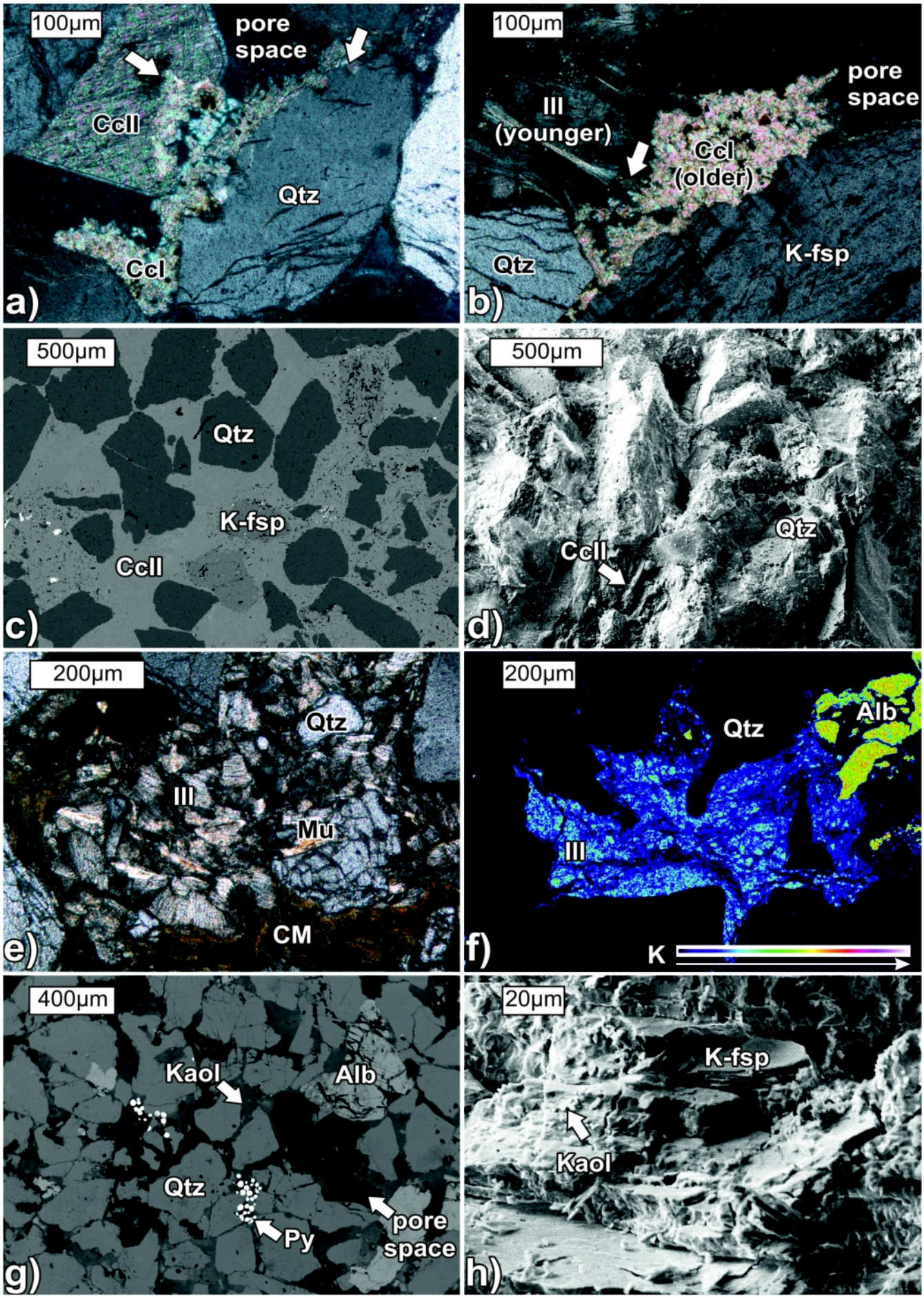
100µm
pore space
CclI
Qtz
Ccl
a)
100µm
pore space
Ill (younger)
Ccl (older)
Qtz
K-fsp
b)
500µm
Qtz
K-fsp
CclI
c)
500µm
Qtz
CclI
d)
200µm
Qtz
Ill
Mu
CM
e)
200µm
Qtz
Alb
Ill
K
f)
400µm
Kaol
Alb
Qtz
Py
pore space
g)
20µm
K-fsp
Kaol
h)

Van Berk, 2009). Thus, the composition of the organic fraction itself and the change of pH and Eh conditions in pore waters are affected by degradation reactions during organic matter decomposition. This may trigger dissolution of primary minerals and precipitation of cements. Furthermore, the organic substance is also a source of ions, which is mainly carbon, available for reactions. Two extreme endmembers and any combination thereof are available for organic matter degradation: (i) organic matter $C^{(0)}H_2O$ degrades in anoxic conditions into $C^{(IV-)}H_4$ and thus result in a consumption of H^+ (increase in pH) and (ii) when free oxygen or oxidizing agents such as iron or manganese oxides are present $C^{(0)}H_2O$ reacts to $C^{(IV+)}O_2$. This results in the release of $4H^+$ per mole CH_2O and thus in pH decrease (Schulz et al., 2009; Schulz & Van Berk, 2009).

The observed diagenetic minerals are used as the basis for the following interpreted post-depositional processes (Fig. 13). The influence of the depositional environment on the sediment petrology and thus on detrital particles (siliciclastics: mainly quartz and feldspar, mica and clay minerals; Fig. 13a,b) is already discussed above. Generally, a mixture of variable minerals from different source areas was deposited in the sediment package, which was not in thermodynamic equilibrium. The ensuing diagenetic processes headed for more stable minerals, following the rules of thermodynamic and kinetic (Bjørlykke et al., 2014). Thereby pore water acted as agent for mass transport (Taylor et al., 2010):

5.2.2 Eogenesis

5.2.2.1 Oxidation and nitrate reduction

Diagenetic processes started immediately after deposition. Synsedimentary oxygen and later nitrate reduction initiated a reduced setting (Froelich et al. 1979; Einsele, 2000; Schulz et al., 2009) (Fig. 13a). The nitrate reduction is accompanied with manganese and adjacent iron reduction. The electrochemical potential moves from positive to negative and enables the solution of Mn- and Fe-oxides and hydroxides by reduction. In that way, electron acceptors are formed to support nitrate oxidation (Froelich et al., 1979). Furthermore, alkaline conditions are induced, because of H^+ depletion (Hesse & Schacht, 2011).

Figure 9: Diagenetic features of sandstones from the Ampfing Formation: Thin section photographs of a) different cement generations and b) paragenetic relationship of corroded calcite (older) and illite ~~kaolinite~~ (younger) in water-bearing sandstones. c) Back scatter electron (BSE)-image of "cement"-supported texture and dissolved alkali feldspar of strongly cemented sandstones. d) SEM-image of sparitic calcite cement CcII, covering minerals of strongly cemented sandstones; note the low porosity of the strongly cemented sample. e) Paragenetic relationship of clay mineral accumulations along the margins of former open pore space (old) and the pore space filling illite ~~kaolinite~~ (young) and f) WDX element mapping of K in oil-bearing sandstones. g) BSE-image of kaolinite enclosing detrital grains in a gas-bearing sandstone. h) SEM-image of kaolinite booklets, which grow on the surface of alkali feldspar in gas-bearing sandstones (CM: clay minerals; Alb: albite).

Authigenic minerals: Eogenetic processes comprise the formation of glauconite and clay minerals (Fig. 13b):

Glauconite – The reduced setting is a commonly cited requisite for glauconitic mineral precipitation (Füchtbauer, 1988) in the Ampfing Formation (Fig. 8e). These glauconite pellets formed at the sediment-water interface in the shallow-marine realm (Porrenga, 1957). K^+ and Fe^{2+}, a prerequisite for the formation of these minerals, was derived from seawater (Meunier & El Ablani, 2007).

Clay minerals – A fraction of clay minerals was derived from detrital fine-grained sediments. Detrital and authigenic clay minerals, and some iron hydroxides and/or mixture of organic and inorganic undifferentiated fine-grained matrix, built overgrowths on detrital grains or formed as in-situ alteration products (e.g. Figs. 9e,f). Gier et al. (1998, 1999) identified detrital illite, chlorite, and kaolinite in the <0.2µm fraction of pelitic sediments (Eocene-Miocene) in the NAFB. They emphasize the abundance of kaolinite within the Eocene layers. The immediate kaolinite growth in the secondary pores of the corroded feldspar grain (e.g. Fig. 11a), suggests an eodiagenetic formation of this clay mineral. But also the partial dissolution of the metamorphic lithic fragments and mica enabled the liberation of ions, such as Mg^{2+}, Mn^{2+} and Fe^{2+}. Eogenetic clay minerals of Eocene sandstones comprise smectite, (e.g. Figs. 11a,f), and minor amounts of kaolinite and chlorite. The formation of the particular clay mineral type depends on the availability of the cations and of the pH of the solution. Pore water can be either (i) diluted by fresh meteoric water, which is less concentrated in ions and thus acidic, or (ii) derived from sea-water, which is higher concentrated and alkaline (Hurst & Irwin, 1982). According to the constant high pH, which is buffered by feldspar dissolution, and the concentration of cations dissolved in the pore water during the eogenesis of Eocene sandstones, the formation of 2:1 clay type smectite was favored (e.g. Kerr, 1952; Hurst & Irwin, 1982; Wilson et al., 2014). Eogenetic kaolinite formed by feldspar disintegration in absence of K^+. The disintegration of albite minerals supplied Na for smectite growth. Accordingly, smectite is the most prominent eogenetic clay mineral in the shallow marine Ampfing Formation.

5.2.2.2 Sulfate reduction

When O and NO_3^- are consumed, SO_4^{2-} reduction commences (Fig. 13a). Sulfate reduction and methanogenesis are the predominating processes during burial diagenesis (Froelich et al., 1979; Einsele, 2000). Continuing microbial activity and reduction of Fe^{3+} increases pore water alkalinity (Machel & Mountjoy, 1986; Curtis, 1978). The microbial-produced carbon is suggested as the source for carbonate cements (Curtis et al., 1977). Diagenetic processes of the intermediate to deep burial are buffered (e.g. Smith & Ehrenberg, 1989; Land & Macpherson, 1992; Hutcheon et al., 1993; Giles, 1997). These geochemical reactions encompass aluminosilicates and carbonate minerals and control the evolution of the pore fluids (Taylor et al., 2010). Thus for example, the partial feldspar dis-

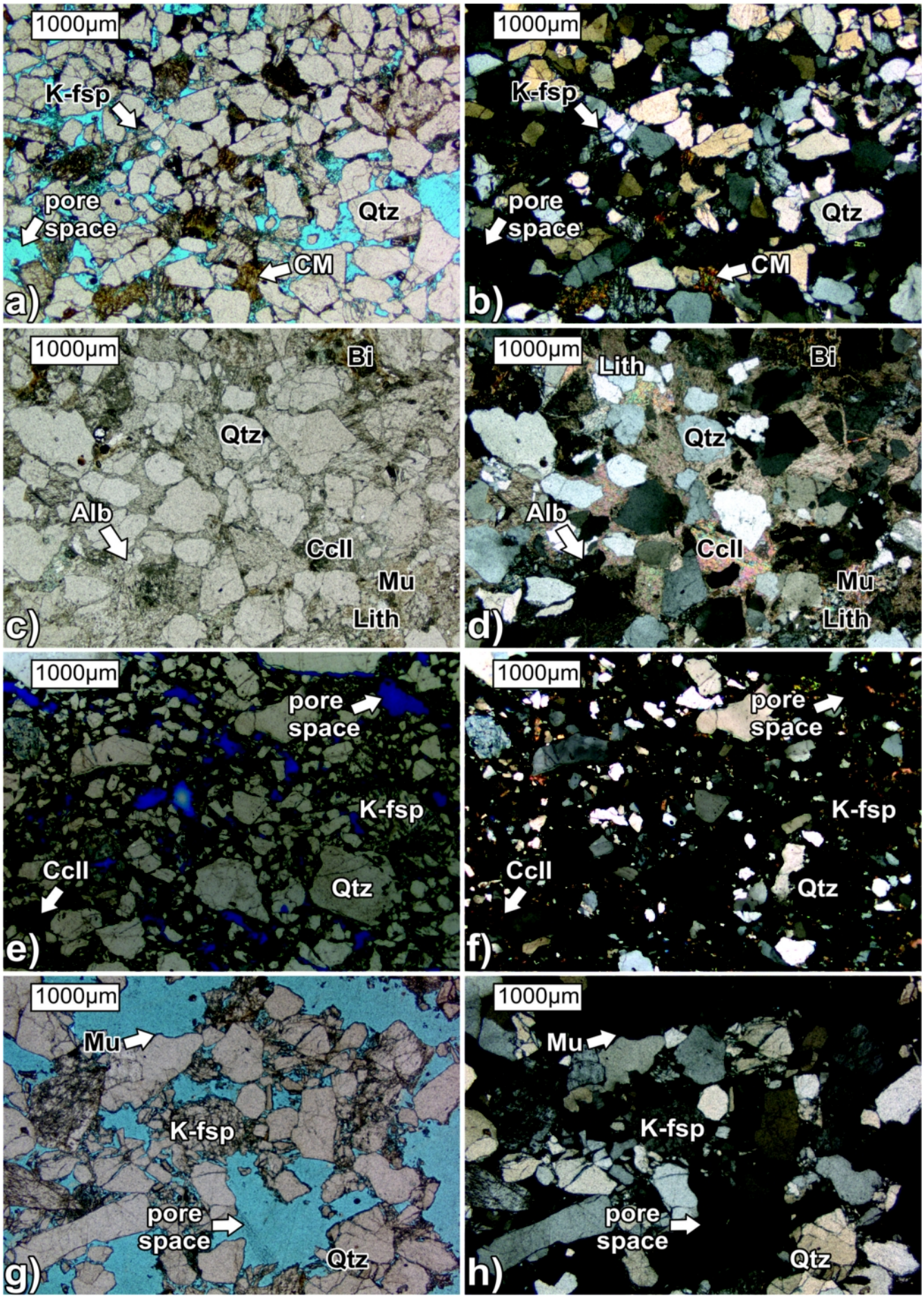
1000µm
K-fsp
pore space
Qtz
CM
a)
1000µm
K-fsp
pore space
Qtz
CM
b)
1000µm
Bi
Qtz
Alb
CclI
Mu
Lith
c)
1000µm
Lith
Bi
Qtz
Alb
CclI
Mu
Lith
d)
1000µm
pore space
K-fsp
CclI
Qtz
e)
1000µm
pore space
K-fsp
CclI
Qtz
f)
1000µm
Mu
K-fsp
pore space
Qtz
g)
1000µm
Mu
K-fsp
pore space
Qtz
h)

solution was important for the eogenetic microbial activity. Since this process holds the pH of the pore water constant via buffering, carbonate precipitation was favored (Van Berk et al., 2009). The free Ca^{2+} from anorthite was a possible supplementary substitute for carbonate formation (Van Berk et al., 2009), next to the common Ca-sources as sea water, fossils or detrital limestone. In the bicarbonate buffer system, carbonate species were produced by the buffering effect of feldspar dissolution (Van Berk et al., 2009). The bicarbonate buffer system comprises the carbonate species: carbonic acid (CO_3^{2-}), bicarbonate ion (HCO_3^-), and carbon dioxide (CO_2). The presence of the prevailing species is dependent on the pH of the pore water. Under alkaline conditions (pH > 7) bicarbonate and carbonic acid are predominant. With increasing pH (pH > 10.3) the CO_3^{2-} occupies the dominant position (e.g. Appelo & Postma, 2005). In the case of the Eocene sandstones, microbial produced carbon (C^{4+}) build chemical compounds, such as carbonate species in the pore water. The microbial stimulated alkaline conditions result in the presence of HCO_3^- and later CO_3^{2-}. The generation of these carbonate species might result in the oversaturation with regard to calcite (Fu, 2014), leading to carbonate precipitation (Curtis et al., 1977).

Authigenic minerals:

Calcite – The first carbonate generation is represented by micritic calcite (CcI) (Fig. 13b). Later, sparitic cement (CcII) partly replaced the micrite (Fig. 9a). These cement generations (CcI and CcII) are associated with the eogenetic stage of sulfate reduction. Eogenetic carbonate dissolution and cementation are common processes, because carbonate depicts comparably fast reaction rates at low temperatures and shallow depths (Bjørlykke et al., 2014). The open pore space was significantly reduced due to these early cementation phases. Less cemented sandstones of the Voitsdorf Formation and the Cerithian Beds belong to the carbonate isotope group 1 and show a $\delta^{13}C$ ratio between -5.9 to +2.2‰ [VPDB] and a $\delta^{18}O$ ratio between -8.3 to -4.3‰ [VPDB] (Fig. 12). $\delta^{13}C$ ratios are similar to carbonates of sea water. $\delta^{18}O$ ratios exhibit a slight negative shift reflecting the primary fluviatile to brackish depositional setting and thus, are evidence for the eogenetic formation of the cements in these sediments.

Siderite – In fluviatile (Voitsdorf Formation) and tidal (Cerithian Beds) settings, siderite formed within biotite flakes (Fig. 11a; 13b), which provided the necessary Fe^{2+}. The formation of siderite requires suboxic to reducing environments with low sulphide concentrations (Hammer et al., 2010). The low amount of pyrite (1 vol%) in investigated samples supports the low sulphide concentration.

Figure 10: Thin section photographs in plane- and cross-polarized light of different samples from the Voitsdorf Formation: a,b) one sample from the oil-bearing sandstone; c,d) one sample from the cemented sandstone. Thin section photographs of different samples from the Cerithian Beds: e,f) one sample from the oil-bearing sandstone; g,h) one sample from the gas-bearing sandstone (Lith: lithic fragment; Bi: biotite). Note high porosity in a,b,e,f,g,h. Please note that the high porosity on this figure is a preparation artifact.

Detritus corrosion – Carbonate generation was accompanied by partial dissolution of siliciclastic minerals (feldspar and to some extent quartz) in all investigated sandstones (Fig. 13b). Kashik (1965) and Friedman & Sanders (1978) suggested a dissolution of quartz at a pH > 9. The release of silica (SiO_2) supported the formation of authigenic silicate minerals, such as clay mineral, and subordinately microcrystalline quartz. In general, quartz cementation is controlled by the kinetic of quartz reactions and thus dependent on the Si concentration and temperature (Walderhaug, 1996). However, the kinetic reaction rates of silicate are very slow at shallow depths (Bjørlykke et al., 2014). The dissolution of the instable feldspar type anorthite is suggested to start the first, because of its higher CO_2 buffering capacity (Van Berk et al., 2009). Thereby, Si^{4+}, Al^{3+}, and Ca^{2+} ions were released and became available for further reactions. Within the Eocene samples, only a low amount of anorthite minerals were observed and are suggested to be dissolved during the early stages of diagenesis largely. The dissolution of anorthite stabilizes the pH of pore water on a high level (Van Berk et al., 2009; 2013; Fu, 2014). Therefore the feldspars albite and K-feldspar do not show this strong dissolution features as anorthite. Albite and K-feldspar are disintegrating and partly dissolved within the Eocene sandstones. K-feldspar grains are more stable than albite. This is because of the higher buffering capacity of albite compared to K-feldspar (Van Berk et al., 2009). Albite dissolution released the elements Si^{4+}, Al^{3+}, and Na^{2+}, whereas partial K-feldspar dissolution allocated Si^{4+}, Al^{3+} and K^+ ions. The processes of feldspar dissolution proceeded during the entire diagenetic history of Eocene reservoir rocks and were an essential ion source for further authigenic mineral formations. The dissolution of feldspar is frequently concomitant with the precipitation of clay minerals, as discussed already above and exemplified in Fig 11a. The released ions, dissolved within the pore water, were incorporated into authigenic hydrous aluminum phyllosilicates.

5.2.2.3 Mesogenesis

5.2.2.3.1 Sulfate reduction (advanced stage)

The initial $\delta^{13}C$ pool ($\delta^{13}C$: ±0‰ [VPDB]), the carbon source for Eocene carbonate cements, was gradually depleted in ^{13}C due to microbial metabolization of organic matter during diagenesis (Hesse & Schacht, 2011). The eodiagenetic zone of bacterial oxidation has a low impact on the isotope fractionation, whereas sulfate reduction results in the progressive lowering of the $\delta^{13}C$ values (see Fig. 12). Based on carbonate isotopy, an eodiagenetic stage of sulfate reduction ($\delta^{13}C$: 0 to -15‰) and an advanced stage of sulfate reduction ($\delta^{13}C$: > -25‰) can be distinguished (e.g. Claypool & Kaplan, 1974; Irwin et al., 1977; Curtis, 1978; Gluyas, 1983, 1984; Allan & Wiggins, 1993) (Fig. 13a).

Authigenic minerals:

Carbonate cementation – The advanced stage of bacterial

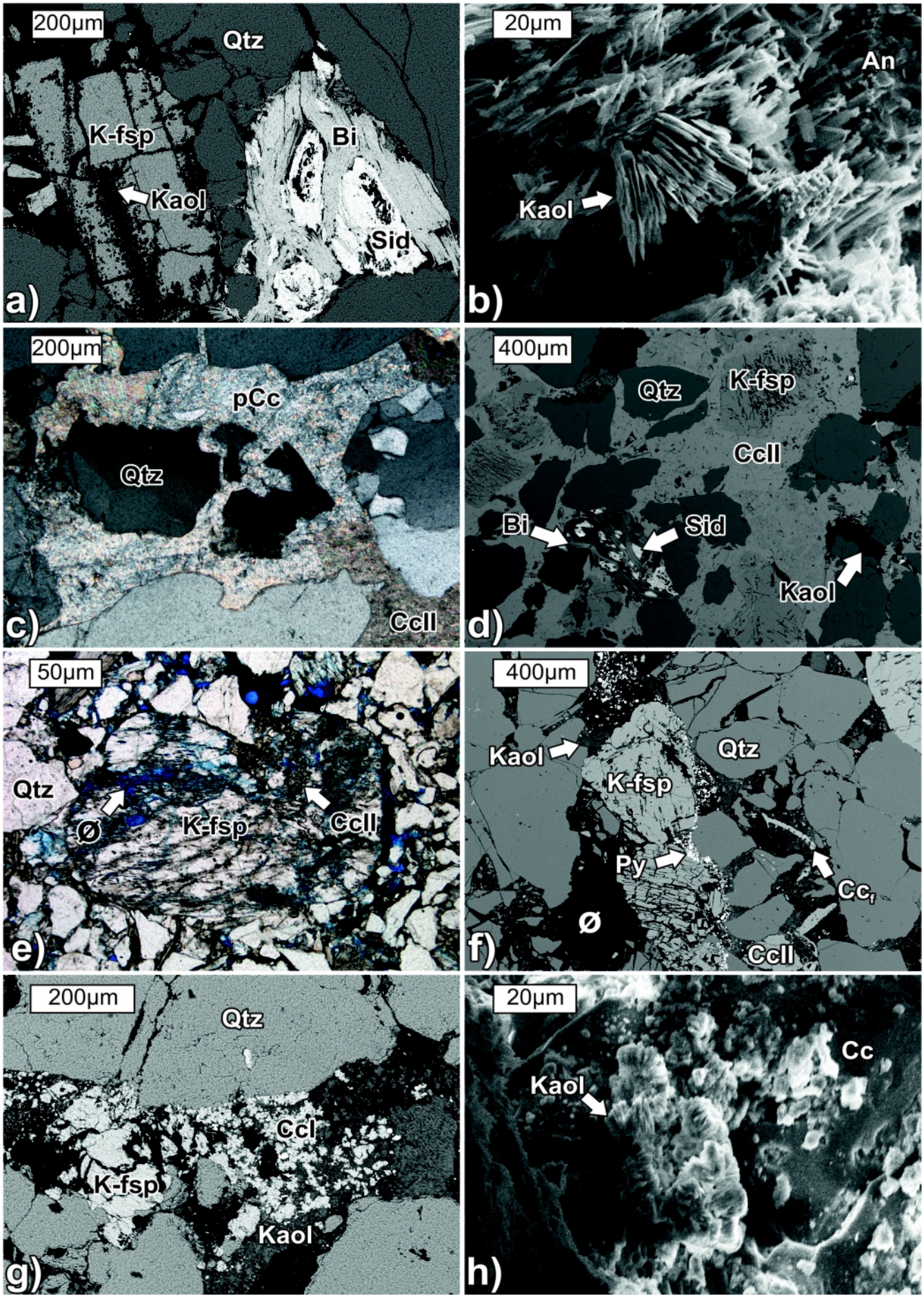
200µm
Qtz
K-fsp
Bi
Kaol
Sid
a)
20µm
An
Kaol
b)
200µm
pCc
Qtz
CcII
c)
400µm
Qtz
K-fsp
CcII
Bi
Sid
Kaol
d)
50µm
Qtz
Ø
K-fsp
CcII
e)
400µm
Kaol
Qtz
K-fsp
Py
Cc$_f$
Ø
CcII
f)
200µm
Qtz
Ccl
K-fsp
Kaol
g)
20µm
Cc
Kaol
h)

sulfate reduction is recorded by strongly cemented sandstone samples within the water-bearing zone (Figs. 8c,d; 9c,d) as well as with very light $\delta^{13}C$ values (-28.4 to -22.2‰) and moderately light $\delta^{18}O$ ratios (-8.4 to -7.9 ‰) (Watson, 1995) (Fig. 12; 13b). The ratios are similar to those observed in strongly cemented sandstone samples from Cerithian Beds ($\delta^{13}C$: -27.3 to-10.1 ‰, $\delta^{18}O$: -7.3 to -4.0 ‰), which have been described by Sachsenhofer et al. (2006). In general, such light values were derived at the sulfate reduction zone from anaerobic oxidation of organic matter and hydrocarbons (Chien et al., 2012; Watson, 1995). Nevertheless, the authors are aware, that the light $\delta^{13}C$ ratios can also be also derived from a significant contribution of CO_2 generated by oil biodegradation (Donovan, 1974; Irwin et al., 1977; Gould & Smith, 1978; Macaulay et al., 1998; Mazzini et al., 2003). However, the texture of the sediment, indicating an eogenetic formation, can hardly be connected with a telogenetic hydrocarbon emplacement. Depletion of $\delta^{18}O$ ratios may be a sign of the increasing formation temperature of the carbonates (Friedman & O´Neil, 1977; Irwin et al., 1977). These isotopically light carbonates belong to the carbonate isotope group 2. The sparitic cement (CcII-a) shows local recrystallization patterns into poikilitic cement (pCc). A slight Mg enrichment in these pervasive CcII-a is interpreted as an indicator for gradual organic matter conversion (Schulz et al., 2009; Schulz & Van Berk, 2009) in a suboxic setting (Einsele, 2000).

Figure 11: Diagenetic features of sandstones from the Voitsdorf Formation and the Cerithian Beds: a) BSE-image of siderite in biotite and disintegrating alkali feldspar with kaolinite growth (oil-bearing sandstone; Voitsdorf Fm.). b) SEM-image of kaolinite, growing on ~~calcite cement~~ feldspar into pore space (oil-bearing sandstone; Voitsdorf Fm.). c) Corroded quartz grains floating in carbonate cement, with partially poikilitic (pCc) character (cemented sandstone; Voitsdorf Fm.). d) BSE-image of the mineral assemblage siderite in biotite, encased within complete calcite cementation (cemented sandstone; Voitsdorf Fm.). Note the alkali feldspar replacement by calcite and the corroded rims of quartz grains. e) Disintegration and replacement of alkali feldspar by calcite and generation of secondary porosity (oil-bearing sandstone; Cerithian Bds.). f) Interstices of detrital grains (quartz and feldspar) filled with pyrite and kaolinite (oil-bearing sandstone; Cerithian Bds.). g) Paragenetic relationship of corroded calcite cement (Ccl, old) and pore space filling kaolinite (young) (gas-bearing sandstone; Cerithian Beds). h) SEM-image of kaolinite (gas-bearing sandstone; Cerithian Beds) (Sid: siderite; pCc: poikilitic calcite, Ccf: calcite from fossil).

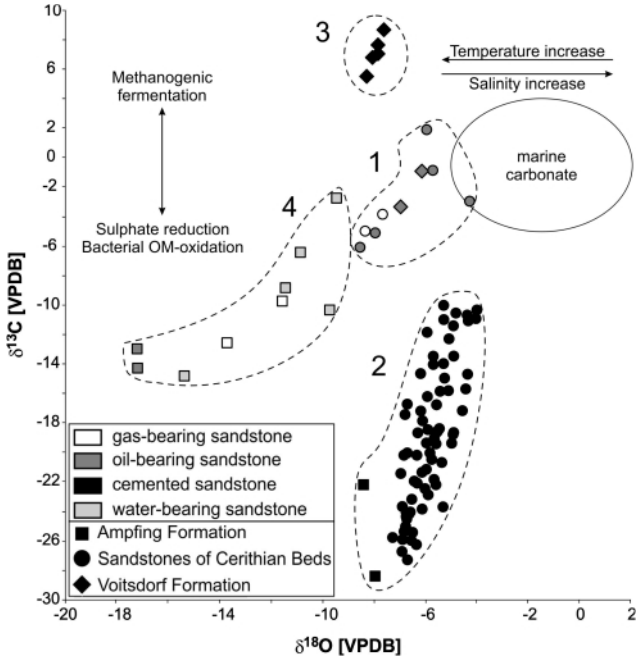

Figure 12: Plot of carbon and oxygen stable isotopic composition of bulk carbonates from investigated sandstones. Typical values for marine carbonates (after Dimitrakopoulus & Muehlenbachs, 1987) are shown for comparison. Influence of salinity and temperature, as well as methanogenic fermentation and bacterial sulphate reduction after Allan & Wiggins (1993). (OM: organic matter)

Clay mineral alteration – During diagenesis, eogenetic clay minerals altered into more stable clay minerals (Bjørlykke et al., 1989, 2014), involving illite or chlorite (Fig. 13b). Depending on the availability of ions (K^+, Al^{2+}, Na^{2+}, Ca^{2+}, Mg^{2+}, Fe^{3+}, Si^{4+}, OH^-), which were released from the partial dissolution of minerals (especially aluminosilicates) during mesogenesis, a particular type of clay mineral formed. The alteration of kaolinite and smectite in illite or chlorite depends on the availability of Fe^{3+} and Mg^{2+} cations. Hower et al. (1976) and Hoffman & Hower (1979) suggested a temperature of 60 - 100°C for the alteration of smectite in illite. Eogenetic kaolinite and smectite serve as a source of ions (e.g. K^+, Al^{2+}, Na^{2+}, Si^{4+}) and can be transformed in chlorite (Mg-rich penninite) by the aid of Fe^{3+} and Mg^{2+} originating from the corrosion of iron oxides (Velde, 1984) and Fe-, and Mg-rich lithic fragments, and glauconite in the Ampfing Formation, respectively. Illite formed as the most common mineral within investigated Eocene sandstones (e.g. Fig. 9f). Detailed investigations on the clay mineralogy and diagenesis of fine-grained sediments (Eocene-Miocene) in the NAFB reveal a gradual illitization of eodiagenetic mixed-layer illite-smectite with depth (Gier et al., 1998; 1999). Smectite is conversed to illite through I/S mixed-layer intermediate phases. This is related to an incorporation of Al^{2+}- and K^+-ions, probably released by K-feldspar dissolution (Hower et al., 1976; Horton et al., 1985). The transformation is dependent on temperature, and period since burial (Hower et al. 1976). Randomly oriented I/S mixed-layers are still predominant to a depth of up to 2500 m. For this reason a low geothermal gradient of the NAFB (2.9°C / 100 m) is suggested (Gier et al., 1998; 1999). Based on the predominance of illite in the clay mineral fraction in the Eocene sandstones, it can be assumed that a certain proportion of detrital muscovite and eodiagenetic smectite and kaolinite were alterated into the more stable illite. Therefore, some of the big illite booklets (70 µm) in the gas-bearing sandstones of the Ampfing Formation are suggested to be alterated muscovite.

5.2.2.4 Methanogenesis

Sulfate reduction leads into methanogenesis, when sulfate is depleted (Fig. 13a). Organic matter is metabolized by microbial

fermentation and CO_2 is reduced (Whiticar, 1999; Einsele, 2000; Campbell, 2008). The carbonate cement, which precipitates in this zone, incorporates the Carbon originating from reduced CO_2. Timing and depth of these processes are hard to define. Inagaki et al. (2015), for example, observed microbial methanogenesis in a depth of 1700 to 2000 m below sea floor.

Authigenic minerals:

Carbonate cementation – The zone of methanogenesis is indicated by positive $\delta^{13}C$ values. Heavy ^{13}C is derived from fermentation (Irwin et al., 1977; Watson et al., 1995; Einsele, 2000) and carbonate reduction (Whiticar, 1999) during microbial methanogenesis (Carvalho et al., 1995; Einsele, 2000; Schulz & Van Berk, 2009). The initial presence of free Fe^{2+} in the pore waters enables the incorporation of the reduced (ferrous) form of iron into carbonate minerals. Carbonates with such characteristics have been observed exclusively within strongly cemented sandstones of the oil-bearing zone in well F (CcII-b) (Figs. 4; 5a; 10c,d). Samples from this section show positive $\delta^{13}C$ (+5.5 to +8.7 ‰) and moderately light $\delta^{18}O$ (-8.3 to -7.6 ‰) ratios (carbonate isotope group 3 Fig. 12). In addition, the comparatively tighter texture of the strongly cemented sandstone in the oil-bearing zone suggests a later diagenetic formation of the carbonate minerals (Fig. 13b). The sparitic cements (CcII-b) grade locally into poikilitic cement (pCc) (Fig. 11c). pCc was observed within the isotopically light CcII-a and heavy CcII-b and therefore it is suggested that this recrystallization does not cause a shift in isotopic composition.

Carbonate cement minerals of group 3 may be connected to a paleo-oil-water contact (OWC). Some glauconite pellets altered within hydrocarbon-bearing sandstones at the shallow-marine Ampfing Formation. Fu et al. (2015) related glauconite alteration in reservoir rocks to oil biodegradation. However, oil within the Eocene reservoir shows no sign of biodegradation (Gratzer et al., 2011). Bacterial activity triggered alkaline conditions and carbonate precipitation especially at the OWC (Machel & Mountjoy, 1986; Watson et al., 1995). A Karpatian/Badenian westward tilting and an uplift especially in the eastern part during late Miocene of the NAFB is evident (Gusterhuber, 2012), which may have induced a displacement of primary OWCs.

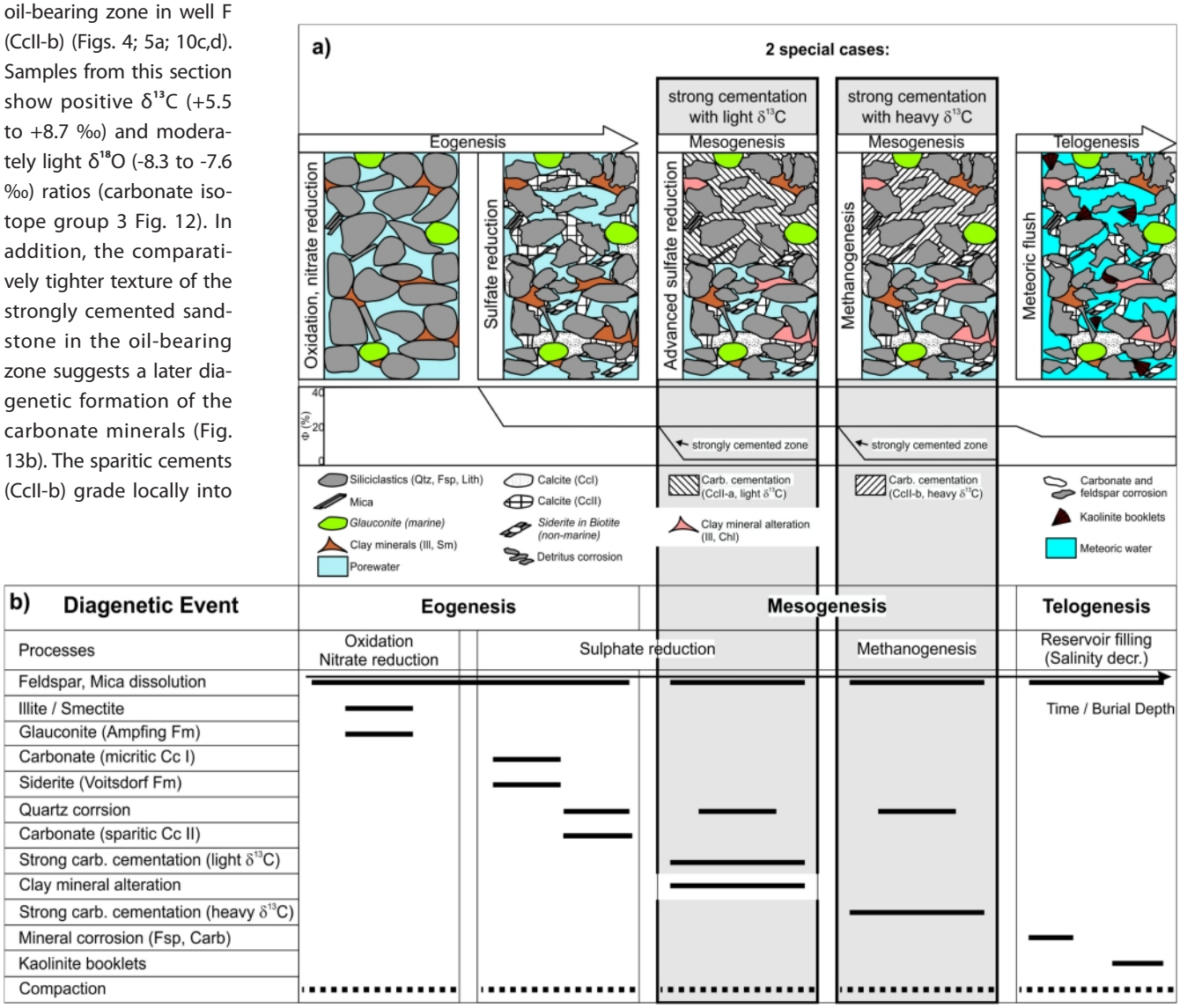

Figure 13: a) Conceptual model of the diagenetic history of Eocene sandstones, which bear water-, oil and gas. b) Schematic paragenetic sequence of diagenetic events in Eocene sandstones based on petrofabric evidence. The two described special cases of the strong carbonate cementation at water- and oil-bearing zones are highlighted in the framed boxes. Please note that the clay mineral alteration during mesogenesis is related to all reservoir units, irrespective of their pore filling (water/oil/gas/cement).

5.2.3 Telogenesis

5.2.3.1 Meteoric flush

A telogenetic dilution by meteoric water in Eocene reservoir sandstones is provided by hydrochemical data, which prove a late Pleistocene meteoric origin of some formation waters (Andrews et al., 1987) (Fig. 13a). The meteoric flush influenced the lateral and continuous Ampfing Formation more strongly than the underlying Voitsdorf Formation and Cerithian Beds and overprinted the original isotopic composition.

Authigenic minerals:

Carbonate and feldspar corrosion - The detrital feldspar grains and authigenic carbonate cements display some corrosion marks, by etched margins, in all reservoir units (Fig. 11g; 13b). Additionally, carbonate cements (CcI and CcII) from the less cemented sandstones of the Ampfing Formation are characterized by $\delta^{13}C$: -14.8 to -2.8 ‰ and $\delta^{18}O$: -17.2 to -9.4 ‰ ratios (carbonate isotope group 4) (Fig. 12). These values show a trend towards lighter isotope ratios independent from their fluid content (gas/oil/water). The depletion of ^{18}O relative to a marine setting might be due to meteoric flush (Dimitrakopoulus & Muehlenbachs, 1987; Watson et al., 1995). The lighter $\delta^{13}C$ ratios are attributed to a proceeding sulfate reduction. Petrographically cements (CcI and CcII) of carbonate isotope group 4 resemble that of group 1, but belong to a different facies. Therefore, the carbonate cements of group 4 exhibit different isotopic compositions from the formation of carbonate cementation at the onset.

Kaolinite booklets - Kaolinite precipitation indicate a lowering in the pH of the fluid phase, which suggests a meteoric flush (Bjørlykke & Brendsdal, 1986; Bjørlykke et al., 1989; Bjørkum et al., 1990) (Fig. 13b). Kaolinite was formed by partial dissolution of Al-rich silicate minerals, mainly feldspar. It often grows on older clay mineral accumulations (illite, smectite). Further, the kaolinites developed in older secondary pores of authigenic cements. Lanson et al. (2002) and Hammer et al. (2010) emphasized that meteoric flush removes ions, amongst others K^+, from the system and, hence, promotes kaolinite rather than illite precipitation. It is also suggested, that Si^{4+} was removed and diluted, respectively, because no quartz- or feldspar overgrowths have been observed. Authigenic kaolinite formation distinguishes itself by euhedral booklets geometry and intercrystalline micropores filling with kaolinite with a mean size of about 20 µm (Hurst & Nadeau, 1995; Ketzer et al., 2009). Kaolinite formation is accompanied by pore space reduction.

6. Conclusions

The present study contributes to the understanding of the relation between hydrocarbon accumulation and pore space evolution in Eocene reservoir units from the NAFB. Voitsdorf Formation, Cerithian Beds and Ampfing Formation mainly host thermogenic hydrocarbons and a small amount of microbial gas.

- The reservoir quality is strongly controlled not only by varying detrital input and, hence, the paleogeographic position, but also by the transport distance from the hinterland. Low compositional maturity is associated to high feldspar and as alteration product high clay mineral content, which restricts preferably fluid flow preferably. Primarily, sandstones from the Ampfing Formation show the highest maturity.
- Metabolism of surrounding organic matter-rich clayey marls provided microbial gas. Early diagenetic carbonate precipitation (CcI, CcII) was promoted by bacterially stimulated alkaline conditions. This early cementation reduced the initial pore space and prevented further compaction.
- Calcite cements from the Voitsdorf Formation and the Cerithian Beds show $\delta^{13}C$- and $\delta^{18}O$-values between -5.9 to +2.2‰ and -8.3 to -4.3‰ [VPDB] (carbonate isotope group 1), respectively, which supports a non-marine pore water during calcite precipitation.
- Strongly cemented sandstones from the water-bearing zone show $\delta^{13}C$ ratios (-28.4 to -22.2‰; carbonate isotope group 2) and are locally slightly enriched in Mg (CcII-a). It is suggested that these light ratios are formed in the advanced stage of sulfate reduction.
- Strongly cemented sandstones within the oil-bearing zone exhibit isotopically heavy carbonate cements (carbonate isotope group 3: $\delta^{13}C$ under +8.7‰). Positive isotope values and Fe-enrichment in carbonate cements (CcII-b) are likely associated with fermentation (methanogenesis).
- Telogenesis is characterized by mineral destabilization (e.g. carbonate and feldspar corrosion) and kaolinite precipitation.
- A dilution of formation water (meteoric flush) is indicated by light $\delta^{18}O$ ratios (group 4: -17.2 to -9.4‰) of the carbonate cements from the shallow-marine Ampfing Formation during late diagenesis.

Acknowledgements

Special thanks go to RAG AG for allocating core material and the permission to publish this study. Sincere thanks are given to D. Birgel, S. Gier, and S. Neuhuber (University of Vienna, Department of Geodynamics and Sedimentology) for productive consultations and discussions. Thanks to the technical instructions of P. Onuk (Montanuniversitaet Leoben, Chair of Geology and Economic Geology) for helping with SEM and F. Zaccarini (Montanuniversitaet Leoben, Chair of Resource Mineralogy) for the microprobe analysis. A huge heartfelt thank you to Stephanie Fend, JD for linguistic revision.

References

Appelo, C.A.J. and Postma, D., 2005. Geochemistry, Groundwater and Pollution. Balkema Publisher, Amsterdam, 2nd Edition, 668pp.

Aharon, P., 2000. Microbial processes and products fueled by hydrocarbons at submarine seeps. In: R.E. Riding and S.M.

Awramik (eds.), Microbial Sediments. Springer, Berlin, 270-281. http://dx.doi.org/10.1007/978-3-662-04036-2_29

Allan, J.R. and Wiggins, W.D., 1993. Dolomite reservoirs: Geochemical Techniques for Evaluating Origin and Distribution. American Association of Petroleum Geologists Continuing Education Course Note Series, 36, 170 pp.

Andrews, J.N., Youngman, M.J., Goldbrunner, J.E. and Darling, W.G., 1987. The geochemistry of formation waters in the Molasse Basin of Upper Austria. Environmental Geology and Water Sciences, 10, 43-57.

Bachmann, G. H., Müller, M. and Weggen., K., 1987. Evolution of the Molasse Basin (Germany, Switzerland). Tectonophysics, 137, 77-92.

Bechtel, A., Gratzer, R., Linzer, H.-G. and Sachsenhofer, R. F., 2013. Influence of migration distance, maturity and facies on the stable isotopic composition of alkanes and on carbazole distributions in oils and source rocks of the Alpine Foreland Basin of Austria. Organic Geochemistry, 62, 74-85. http://dx.doi.org/10.1016/j.orggeochem.2013.07.008

Bjørlykke, K., 2014. Relationships between depositional environments, burial history and rock properties. Some Principal aspects of diagenetic processes in sedimentary basins. Sedimentary Geology, 301, 1-14. http://dx.doi.org/10.1016/j.sedgeo.2013.12.002

Bjørlykke, K. and Brendsdal, A., 1986. Diagenesis in the Brent sandstone in the Statfiord field, North Sea. In: D. Gautier (ed.), Roles of Organic Matter in Sediment Diagenesis. SEPM Special Publication, 38, 157-167.

Bjørlykke, K., Ramm, M. and Saigal, G.C., 1989. Sandstone diagenesis and porosity modification during basin evolution. Geologische Rundschau, 78/1, 243-268. http://dx.doi.org/10.1007/BF01988363

Bjørkum, P.A., Mjøs, R., Walderhaug, O. and Hurst, A., 1990. The role of the late Cimmerian unconformity for the distribution of kaolinite in the Gullfaks Field, northern North Sea. Sedimentology, 37/3, 396-406. http://dx.doi.org/10.1111/j.1365-3091.1990.tb00143.x

Brindley, G.W., 1980. Quantitative X-ray mineral analysis of clays. In: G.W. Brindley and G. Brown (eds.), Crystal Structures of Clay Minerals and their X-ray Identification, Mineralogical Society, London, 411-438.

Campbell, K.A., Francis, D.A., Collins, M., Gregory, M.R., Nelson, C.S., Greinert, J. and Aharon, P., 2008. Hydrocarbon seep-carbonates of a Miocene forearc (East Coast Basin), North Island, New Zealand. Sedimentary Geology, 204/3-4, 83-105. http://dx.doi.org/10.1016/j .sedgeo.2008.01.002

Carvalho, M.V., De Ros, L.F. and Gomes, N.S., 1995. Carbonate cementation patterns and diagenetic reservoir facies in the Campos Basin Cretaceous turbidites, offshore eastern Brazil. Marine and Petroleum Geology, 12/7, 741-758. http://dx.doi.org/10.1016/0264-8172(95)93599-Y

Chien, C.W., Huang, C.Y., Chen, Z., Lee, H.C. and Harris, R., 2012. Miocene shallow-marine cold seep carbonate on fold-and thrust Western Foothills, SW Taiwan. Journal of Asian Earth Sciences, 56, 200-211. http://dx.doi.org/10.1016/j.jseaes. 2012.05.013

Claypool, G.E. and Kaplan, I.R., 1974. The origin and distribution of methane in marine sediments. In: Kaplan, I. R. (Ed.) Natural Gases in Marine Sediments. Marine Sciences, 3, 99-140.

Curtis, C.D., 1978. Possible links between sandstone diagenesis and depth related geochemical relations occurring in enclosing mudstones. Journal Geological Society London, 135, 107-117. http://dx.doi.org/10.1144/gsjgs.135.1.0107

Curtis, C.D., Burns, R.G. and Smith, J.V., 1977. Sedimentary geochemistry: environments and processes dominated by involvement of an aqueous phase (and discussion). Philosophical Transactions of the Royal Society of London, Series A, Mathematical and Physical Sciences, 286/1336, 353-372. http://dx.doi.org/10.1098/rsta.1977.0123

Dimitrakopoulus, R. and Muehlenbachs, K., 1987. Biodegradation of petroleum as a source of 13C-enriched carbon dioxide in the formation of carbonate cement. Chemical Geology, 65/3-4, 283-291. http://dx.doi.org/10.1016/0168-9622(87)90008-X

Donovan, T.J., 1974. Petroleum microseepage at Cement, Oklahoma-evidence and mechanism. American Association of Petroleum Geologists Bulletin, 58/3, 429-446.

Einsele, G., 2000. Sedimentary Basins: Evolution, Facies, and Sediment Budget. Springer, 792 pp. http://dx.doi.org/10.1007/978-3-662-04029-4

Folk, R.L., 1974. Petrology of sedimentary rocks. Hemphill, Austin, 107pp.

Friedman, I. and O´Neil, J.R., 1977. Compilation of stable isotope fractionation factors of geochemical interest. In: M. Fleischer (ed.), Data of Geochemistry. US Geological Survey Professional Paper, 440-KK, 6th edition.

Friedman, G.M. and Sanders, J.E., 1978. Principles in Sedimentology. Wiley, 792pp. http://dx.doi.org/10.1002/esp.3290040317

Froelich, P.N., Klinkhammer, G.P., Bender, M.L., Luedtke, N.A., Heath, G.R., Cullen, D., Dauphin, P., Hammond, D., Hartman, B. and Maynard, V., 1979. Early oxidation of organic matter in pelagic sediments of the eastern equatorial Atlantic: suboxic diagenesis. Geochimica et Cosmochimica Acta, 43/7, 1075-1090. http://dx.doi.org/10.1016/0016-7037(79)90095-4

Fu, Y., 2014. Development and Application of Numerical Modeling for Evaluating and Predicting Hydrogeochemical Processes Temporally and Spatially Evolving in Petroleum Reservoirs: Case Studies: Miller Oilfield (UK North Sea) and Siri Oilfield (Danish North Sea). Ph.D. thesis, Clausthal University of Technology, Germany, 213pp.

Fu, Y., Van Berk, W., Schulz, H.M. and Mu, N., 2015. Beritherine formation in reservoir rocks from the Siri oilfield (Danish North Sea) as result of fluid-rock interactions: Part II. Deciphering organic-inorganic processes by hydrogeochemical modeling. Marine and Petroleum Geology, 65, 317-326. http://dx.doi.org/10.1016/j.marpetgeo.2015.01.007

Füchtbauer, H., 1988. Sediment-Petrologie. Teil. II: Sedimente und Sedimentgesteine. Schweizerbart, Stuttgart, 1141 pp. http://dx.doi.org/ 10.1007/3-540-27405-7_23

Gier, S., 1998. Burial diagenetic processes and clay mineral

formation in the Molasse Zone of Upper Austria. Clays and Clay Minerals, 46, 658-669. http://dx.doi.org/10.1346/CCMN.1998.0460606

Gier, S., 1999. Diagenese pelitischer Sedimente in der Molassezone Oberösterreichs. Mitteilungen der Österreichischen Mineralogsichen Gesellschaft, 144, 45-68.

Giles, M.R., 1997. Diagenesis: A Quantitative Perspective. Kluwer Academic Publication Dordrecht, 526pp.

Gluyas, J.G., 1983. The genesis and diagenesis of shale nodular limestone sequences. PhD. Thesis, University of Liverpool.

Gluyas, J.G., 1984. Early carbonate diagenesis within phanerozoic shales and sandstones the NW European shelf. Clay Minerals, 19, 309-321.

Gould, K.W. and Smith, J.W., 1978. The genesis and isotopic composition of carbonates associated with some Permian Australian coals. Chemical Geology, 24/1-2, 137-150. http://dx.doi.org/10.1016/0009-2541(79)90017-2

Gorenc, M.A. and Chan, M.A., 2015. Hydrocarbon induced diagenetic alteration of the Permian White Rim Sandstone, Elaterite Basin, southeast Utah. American Association of Petroleum Geologists Bulletin, 99/5, 807-829. http://dx.doi.org/10.1306/10081413128

Gratzer, R., Bechtel, A., Sachsenhofer, R.F., Linzer, H.G., Reischenbacher, D. and Schulz, H.M., 2011. Oil-oil and oil-source correlations in the Alpine Foreland Basin of Austria: Insights from biomarker and stable carbon isotope studies. Marine and Petroleum Geology, 28, 1171-1186. http://dx.doi.org/10.1016/j.marpetgeo.2011.03.001

Gross, D., Grundtner, M.L., Misch, D., Riedl, M., Sachsenhofer, R.F. and Scheucher, L., 2015. Diagenetic Evolution and Reservoir Quality of Sandstones in the North Alpine Foreland Basin: A Microscale Approach. Microscopy and Microanalysis, 21/5, 1123-1137. http://dx.doi.org/10.1017/S1431927615014725

Grunert, P., Auer, G., Harzhauser, M. and Piller, W. E., 2015. Stratigraphic constraints for the upper Oligocene to lower Miocene Puchkirchen Group (North Alpine Foreland Basin, Central Paratethys). Newsletters on Stratigraphy, 48/1, 111-133. http://dx.doi.org/10.1016/j.tecto.2004.06.011

Gusterhuber, J., Dunkl, I., Hinsch, R., Linzer, H.G. and Sachsenhofer, R.F., 2012. Neogene Uplift and Erosion in the Alpine Foreland Basin (Upper Austria and Salzburg). Geologica Carpathica, 63, 4, 295-305. http://dx.doi.org/10.2478/v10096-012-0023-5

Gusterhuber, J., Hinsch, R., Linzer, H.-G. and Sachsenhofer, R.F., 2013. Hydrocarbon generation and migration from sub-thrust source rocks to foreland reservoirs: The Austrian Molasse Basin. Austrian Journal of Earth Scienes, 106/2, 115-136.

Gusterhuber, J., Hinsch, R. and Sachsenhofer, R.F., 2014. Evaluation of hydrocarbon generation and migration in the Molasse fold and thrust belt (Central Eastern Alps, Austria), using structural and thermal basin models. American Association of Petroleum Geologists Bulletin, 98, 2, 253-277. http://dx.doi.org/10.1306/06061312206

Hammer, E., Mørk, M.B.E. and Næss, A., 2010. Facies controls on the distribution of diagenesis and compaction in fluvial-deltaic deposits. Marine and Petroleum Geology, 27/8, 1737-1751. http://dx.doi.org/10.1016/j.marpetgeo.2009.11.002

Hesse, R. and Schacht U., 2011. Early Diagenesis of Deep-Sea Sediments. In: H. Hüneke and Th. Mulder (eds.), Developments in Sedimentology, 63, pp. 557-713. http://dx.doi.org/10.1016/B978-0-444-53000-4.00009-3

Hoffman, J. and Hower, J., 1979. Clay mineral assemblages as low-grade metamorphic geothermometers, application to the thrust faulted disturbed belt of Montana, USA. In: P.A. Scholle and R.C. Surdam (eds.), Aspects of diagenesis. SEPM Special publication, 26, 55-79. http://dx.doi.org/10.2110/pec.79.26.0055

Horton, R.B., Johns, W.D. and Kurzweil, H., 1985. Illite diagenesis in the Vienna Basin, Austria. Tschermaks mineralogische und petrographische Mitteilungen, 34, 239-260. http://dx.doi.org/10.1007/BF01082964

Hower, J., Eslinger, E.V., Hower, M.E. and Perry, E.A., 1976. Mechanism of burial metamorphism in argillaceous sediment: 1. Mineralogical and chemical evidence. American Geological Society Bulletin, 87/5, 725-737. http://dx.doi.org/10.1130/0016-7606

Hurst, A. and Irwin, H., 1982. Geological modelling of clay diagenesis in sandstones. Clay Mineralogy, 17, 5-22.

Hurst, A. and Nadeau, P.H., 1995. Clay microporosity in reservoir sandstones: an application of quantitative electron microscopy in petrophysical evaluation. American Association of Petroleum Geologists Bulletin, 79/4, 563-573.

Hutcheon I., Chevalier M. and Abercrombie H.J., 1993. pH buffering by metastable mineral-fluid equilibria and evolution of carbon dioxide fugacity during burial diagenesis. Geochimica et Cosmochimica Acta, 57, 1017-1027. http://dx.doi.org/10.1016/0016-7037(93)90037-W

Inagaki, F., Hinrichs, K.U., Kubo, Y., Bowles, M.W.,Heuer, V. B., Hong, W.L., Hoshino, T., Ijiri, A., Imachi, H., Ito, M., Kaneko, M., Lever, M.A., Lin, Y.S., Methé, B.A., Morita, S., Morono, Y., Tanikawa, W., Bihan, M., Bowden, S.A., Elvert, M., Glombitza, C., Gross, D., Harrington, G. J., Hori, T., Li, K., Limmer, D., Liu, C.H., Murayama, M., Ohkouchi, N., Ono, S., Park, Y.S., Phillips, S.C., Prieto-Mollar, X., Purkey, M., Riedinger, N., Sanada, Y., Sauvage, J., Snyder, G., Susilawati, R., Takano, Y., Tasumi, E., Terada, T., Tomaru, H., Trembath-Reichert, E., Wang, D. T. and Yamada, Y., 2015. Exploring deep microbial life in coal-bearing sediment down to~2.5 km below the ocean floor. Science, 349/6246, 420-424. http://dx.doi.org/10.1126/science.aaa6882

Irwin, H. and Hurst, A., 1983. Applications of geochemistry to sandstone reservoir studies. In: Brooks, J. (Ed.) Petroleum Geochemistry and Exploration of Europe. Geological Society Special Publication, 12, Blackwell, Oxford, 127-146. http://dx.doi.org/10.1144/GSL.SP.1983.012.01.13

Irwin, H., Curtis, C.D. and Coleman, M., 1977. Isotopic evidence for source of diagenetic carbonates formed during burial of organic-rich sediments. Nature, 269, 209-213. http://dx.doi.org/10.1038/269209a0

JCPDS table, 1974. Joint Committee for the Powder Diffraction Standards: Selected Powder Diffraction Data for Minerals. JCPDS, Pennsylvania, USA.

Kashik, S.A., 1965. Replacement of quartz by calcite in sedimentary rocks. Geochemistry International, 2, 133-138.

Kerr, P.F., 1952. Formation and Occurrence of Clay Minerals. Clays and Clay Minerals, 1, 1, 19-32.

Ketzer, J.M., Morad, S., Nystuen, J.P. and De Ros, L.F., 2009. The Role of the Cimmerian Unconformity (Early Cretaceous) in the Kaolinitization and related Reservoir-Quality Evolution in Triassic Sandstones of the Snorre Field, North Sea. In: R.H. Worden and S. Morad (eds.), International Association of Sedimentologists, Special Publication, 34, 361-382. http://dx.doi.org/10.1002/9781444304336.ch16

Land, L.S. and Macpherson, G.L., 1992. Origin of saline formation waters, Cenozoic section, Gulf of Mexico sedimentary basin. AAPG Bulletin, 76, 9, 1344-1362.

Lanson, B., Beaufort, D., Berger, G., Bauer, A., Cassagnabère, A. and Meunier, A. (2002. Authigenic kaolin and illitic minerals during burial diagenesis of sandstones: a review. Clay Minerals, 37/1, 1-22. http://dx.doi.org/10.1180/0009855023710014

Lundegard, P.D., Kharaka, Y.K. and Rosenbauer, R.J., 1992. Petroleum as a potential diagenetic agent: Experimental evidence. In: Y.K. Kharaka and A.S. Maest (eds.), Proceedings of the 7th international symposium on water-rock interaction, 1, Low temperature environments, 7, 329-335.

Macaulay, C.I., Fallick, A.E., McLaughlin, O.M., Haszeldine, R.S. and Pearson, M.J., 1998. The significance of $\delta^{13}C$ of carbonate cements in reservoir sandstones: a regional perspective from the Jurassic of the northern North Sea. In: S. Morad (ed.), Carbonate Cementation of Sandstones. International Association Sedimentologists, Special Publication, 26, 395-408. http://dx.doi.org/ 10.1002/9781444304893.ch17

Machel, H.G. and Mountjoy, E.W., 1986. Chemistry and environments of dolomitisation-a reappraisal. Earth Science Review, 23/3, 175-222. http://dx.doi.org/10.1016/0012-8252(86)90017-6

Malzer, O., Rögl, F., Seifert, P., Wagner, L., Wessely, G. and Brix, F., 1993. Die Molassezone und deren Untergrund. In: F. Brix and O. Schulz (eds.), Erdöl und Erdgas in Österreich. Naturhistorisches Museum Wien und F. Berger, 281-358.

Mazzini, A., Duranti, D., Jonk, R., Parnell, J., Cronin, B.T., Hurst, A. and Quine, M., 2003. Palaeo-carbonate seep structures above an oil reservoir, Gryphon Field, Tertiary, North Sea. Geo-Mar Lett, 23/3, 323-339. http://dx.doi.org/10.1007/s00367-003-0145-y

Meunier, A. and El Albani, A., 2007. The glauconite-Fe-illite-Fe-smectite problem: a critical review. Terra Nova, 19/2, 95-104. http://dx.doi.org/10.1111/j.1365-3121.2006.00719.x

Moore, D.M. and Reynolds, R.C., Jr., 1997. X-Ray Diffraction and the Identification and Analysis of Clay Minerals. Oxford University Press, New York, 2nd edition, 378p.

Nachtmann, W., 1989. Lagerstättengeologisches Modell des Obereozäns im Raum Sattledt (Oberösterreichische Molasse). Geologische Paläontologische Mitteilungen Innsbruck, 16, 213-227.

Porrenga, D.H., 1967. Glauconite and chamosite as depth indicators in the marine environment. Marine Geology, 5/5-6, 495-501. http://dx.doi.org/10.1016/0025-3227(67)90056-4

Prochnow, E.A., Remus, M.V.D. and Ketzer J.M., 2006. Organic - inorganic interactions in oilfield sandstones: Examples from turbidite reservoirs in the Campos Basin, offshore eastern Brazil. Journal of Petroleum Geology, 29/4, 361-380. http://dx.doi.org/10.1111/j.1747-5457.2006.00361.x

Rasser, M.W. and Piller, W.E., 2004. Crustose algal frameworks from the Eocene Alpine Foreland. Palaeogeography, Palaeoclimatology, Palaeoecology, 206/1-2, 21-39. http://dx.doi.org/10.1016/j.palaeo.2003.12.018

Reischenbacher, D. and Sachsenhofer, R.F., 2011. Entstehung von Erdgas in der oberösterreichischen Molassezone: Daten und offene Fragen. Berg- und Hüttenmännische Monatshefte, 156/11, 455-460. http://dx.doi.org/10.1007/s00501-011-0037-9

Roeder, D. and Bachmann, G., 1996. Evolution, structure and petroleum geology of the German Molasse Basin. In: P. Ziegler and F. Horvath (eds.), Peri-Tethys Memoir 2, Structure and Prospects of Alpine Basins and Forelands. Mèmoire du Museum National d´Histoire naturelle, 170, 263-284.

Sachsenhofer, R.F. and Schulz, H.-M., 2006. Architecture of Lower Oligocene source rocks in the Alpine Foreland Basin: a model for syn- and post-depositional source-rock features in the Paratethyan realm. Petroleum Geoscience, 12, 363-377. http://dx.doi.org/10.1144/1354-079306-712

Sachsenhofer, R.F., Gratzer, R., Tschelaut, W. and Bechtel, A., 2006. Characterization of non-producible oil in Eocene reservoir sandstones (Bad Hall Nord field, Alpine Foreland Basin, Austria). Marine and Petroleum Geology, 23/1, 1-15. http://dx.doi.org/10.1144/1354-079306-712

Sachsenhofer, R.F., Leitner, B., Linzer, H.G., Bechtel, A., Coric, S., Gratzer, R., Reischenbacher, D. and Soliman, A., 2010. Deposition, erosion and hydrocarbon source potential of the Oligocene Eggerding Formation (Molasse Basin, Austria). Austrian Journal of Earth Sciences, 103/1, 76-99.

Schmidt, F. and Erdogan, L.T., 1996. Paleohydrodynamics in exploration. In: W. Liebl and G. Wessely, (eds.), Petroleum exploration and production in thrust belts, foreland basins and orogenic basins. European Association of Petroleum Geologists Special Publications, 5, 255-265.

Schulz, H.-M., Sachsenhofer, R.F., Bechtel, A., Polesny, H. and Wagner, L., 2002. The origin of hydrocarbon source rocks in the Austrian Molasse Basin (Eocene - Oligocene transition). Marine and Petroleum Geology, 19, 6, 683-709. http://dx.doi.org/10.1016/S0264-8172(02)00054-5

Schulz, H.M., Van Berk, W., Bechtel, A., Struck, U. and Faber, E., 2009. Bacterial methane in the Atzbach-Schwanenstadt gas field (Upper Austrian Molasse Basin), Part I: Geology. Marine and Petroleum Geology, 26/7, 1163-1179. http://dx.doi.org/10.1016/j.marpetgeo.2008.12.004

Schulz, H.M. and Van Berk, W., 2009. Bacterial methane in the Atzbach-Schwanenstadt gas field (upper Austrian Molasse

Basin), Part II: Retracing gas generation and filling history by mass balancing of organic carbon conversion applying hydrogeochemical modelling. Marine and Petroleum Geology, 26/7, 1180-1189. http://dx.doi.org/10.1016/j.marpetgeo.2008.12.003

Sissingh, W., 1997. Tectonostratigraphy of the North Alpine Foreland Basin: correlation of Tertiary depositional cycles and orogenic phases. Tectonophysics, 282/1-4, 223-256. http://dx.doi.org/10.1016/S0040-1951(97)00221-7

Smith, J.T. and Ehrenberg, S.N., 1989. Correlation of carbon dioxide abundances with temperatures in clastic hydrocarbon reservoirs: relationships to inorganic chemical equilibrium. Marine and Petroleum Geology, 6, 129-135.

Surdam, R.C., Crossey, L.J., Hagen, E.S. and Heasler, H.P., 1989. Organic-Inorganic Interactions and Sandstone Diagenesis. American Association of Petroleum Geologists Bulletin, 73/1, 1-23.

Taylor, T.R., Giles, M.R., Hathon, L.A., Diggs, T.N., Braunsdorf, N.R., Birbiglia, G.V., Kittridge, M.G., Macaulay, C.I. and Espejo, I.S., 2010. Sandstone diagenesis and reservoir quality prediction: Models, myths, and reality. AAPG Bulletin, 94, 8, 1093-1132. http://dx.doi.org/10.1306/04211009123

Tucker, M.E., 1996. Methoden der Sedimentologie. Ferdinand Enke Verlag, Stuttgart, 366pp.

Van Berk, W., Schulz, H.M. and Fu, Y., 2009. Hydrogeochemical modelling of CO2 equilibria and mass transfer induced by organic–inorganic interactions in siliciclastic petroleum reservoirs. Geofluids, 9, 253-262. http://dx.doi.org/10.1111/j.1468-8123.2009.00256.x

Van Berk, W. and Schulz, H.M., 2015. B1-02 Rock and Fluids Properties and Interactions in Hydrocarbon Systems. GeoBerlin, Annual Meeting of DGGV and DMG, 4-7 October 2015, Berlin.

Velde, B., 1984. Transformation of clay minerals. In: B. Duran (ed.), Thermal phenomena in sedimentary basins. International Collequim Bordeaux, June 7-10 1983, 11-116.

Veron, J., 2005. The Alpine Molasse Basin - Review of Petroleum Geology and Remaining Potential. Bulletin für angewandte Geologie, 10/1, 75-86.

Wagner, L., 1980. Geologische Charakteristik der wichtigsten Erdöl- und Erdgasträger der oberösterreichischen Molasse, Teil I: Die Sandsteine des Obereozän. Erdoel-Erdgas-Zeitschrift, 96, 338-346.

Wagner, L.R., 1996. Stratigraphy and hydrocarbons in the Upper Austrian Molasse Foredeep (active margin). In: G. Wessely and W. Liebl (eds.), Oil and gas in Alpidic thrust belts and basins of central and eastern Europe. European Association of Geoscientists and Engineers Special Publication, 5, 217-235.

Wagner, L.R., 1998. Tectono-stratigraphy and hydrocarbons in the Molasse Foredeep of Salzburg, Upper and Lower Austria. In: A. Mascle, C. Puifdefábregas, H.P. Luterbacher, and M. Fernández (eds.), Cenozoic Foreland Basins of Western Europe. Geological Society Special Publications, 134, 339-369.

Walderhaug, O., 1996. Kinetic modelling of quartz cementation and porosity loss in deeply buried sandstone reservoirs. AAPG Bulletin, 80, 731-745. http://dx.doi.org/10.1306/64ED88A4-1724-11D7-8645000102C1865D

Watson, R.S., Trewin, N.H. and Fallick, A.E., 1995. The formation of carbonate cements in the Forth and Balmoral Fields, northern North Sea: a case for biodegradation, carbonate cementation and oil leakage during early burial. Geological Society, London, Special Publications, 94, 177-200. http://dx.doi.org/10.1144/GSL.SP.1995.094.01.13

Welton, J.E., 2003. SEM Petrology Atlas. American Association of Petroleum Geologists Chevron, AAPG Methods in Exploration, 4, 235pp. http://dx.doi.org/10.1306/Mth4442

Whiticar, M., 1999. Carbon and hydrogen isotope systematics of bacterial formation and oxidation of methane. Chemical Geology, 161, 291-314. http://dx.doi.org/10.1016/S0009-2541(99)00092-3

Wilson, M.J., Wilson, L. and Patey, I., 2014. The influence of individual clay minerals on formation damage of reservoir sandstones: a critical review with some new insights. Clay Minerals, 49, 2, 147-164. http://dx.doi.org/10.1180/claymin.2014.049.2.02

Received: 09 September 2016
Accepted: 10 April 2017

Marie-Louise GRUNDTNER[1)*], Doris GROSS[1)], Reinhard GRATZER[1)], David MISCH[1)], Reinhard F. SACHSENHOFER[1)] & Lorenz SCHEUCHER[2)]

[1)] Department of Applied Geosciences and Geophysics, Montanuniversitaet Leoben, 8700 Leoben, Austria;

[2)] Rohoel-Aufsuchungs AG, Schwarzenbergplatz 16, 1015 Vienna, Austria;

[*)] Corresponding author, marielouise.grundtner@gmail.com